

## **Copyright Warning & Restrictions**

The copyright law of the United States (Title 17, United States Code) governs the making of photocopies or other reproductions of copyrighted material.

Under certain conditions specified in the law, libraries and archives are authorized to furnish a photocopy or other reproduction. One of these specified conditions is that the photocopy or reproduction is not to be “used for any purpose other than private study, scholarship, or research.” If a user makes a request for, or later uses, a photocopy or reproduction for purposes in excess of “fair use” that user may be liable for copyright infringement,

This institution reserves the right to refuse to accept a copying order if, in its judgment, fulfillment of the order would involve violation of copyright law.

**Please Note: The author retains the copyright while the New Jersey Institute of Technology reserves the right to distribute this thesis or dissertation**

Printing note: If you do not wish to print this page, then select “Pages from: first page # to: last page #” on the print dialog screen

The Van Houten library has removed some of the personal information and all signatures from the approval page and biographical sketches of theses and dissertations in order to protect the identity of NJIT graduates and faculty.

## ABSTRACT

### IN VITRO DRUG DELIVERY BASED ON A POROUS MEMBRANE-BASED AQUEOUS-ORGANIC PARTITIONING SYSTEM AND ITS ENHANCEMENTS THROUGH MOUSE SKIN

by

Qiuxi Fan

Novel approaches for transdermal drug delivery (TDD) based on a porous membrane-based aqueous-organic partitioning system have been investigated and successful deliveries were observed. Doxycycline hydrochloride (HCl), a polar antibiotic drug with a relatively large molecule weight (MW: 480.1) was studied as a basic model agent. Its controlled release using this technique was studied first. Satisfactory release profiles demonstrate the practical potential of such a system to achieve useful controlled release rates. The enhancer linoleic acid was essential to successful release using a mouse skin beneath a porous polymeric membrane. The transport rates of smaller molecules e.g., caffeine and nicotine from the same system without any enhancer were very high. Iontophoretic TDD was studied next using a porous polymeric conducting membrane of polyaniline (PANi). Doxycycline HCl, lidocaine HCl (MW: 271) and caffeine (MW: 194) in their aqueous solutions were model agents. Excellent release profiles were achieved; the conducting PANi membrane appeared to be capable of not only replacing the Ag part of Ag|AgCl electrode system but also providing an additional control over agent transport rate. Aqueous-organic partitioning system was tested with this novel technique as well. Because of the rather low porosity of synthesized PANi membrane, such a system did not yield a high release rate. The transport rates through polymeric membrane alone were accurately predicted using simplified mass transport models for

both iontophoretic and non-iontophoretic systems. Finally, a further application of this new technique was investigated using a thermo-sensitive TDD system. A hydrophilic porous PVDF membrane immobilized with a thermo-sensitive polymeric gel, poly(N-isopropylacrylamide) (PNIPAAm)-*co*-2mol% acrylic acid (AA), demonstrated its release-“on/off” switch function: at normal skin temperature, no release of doxycycline HCl through the skin occurred; under fever condition, certain amount of this antibiotic accumulated beneath the skin.

**IN VITRO DRUG DELIVERY BASED ON A POROUS MEMBRANE-BASED  
AQUEOUS-ORGANIC PARTITIONING SYSTEM AND ITS ENHANCEMENTS  
THROUGH MOUSE SKIN**

by  
**Qiuxi Fan**

**A Dissertation  
Submitted to the Faculty of  
New Jersey Institute of Technology  
In Partial Fulfillment of the Requirements for the Degree of  
Doctor of Philosophy**

**Interdisciplinary Program in Materials Science and Engineering**

**January 2005**

Copyright © 2005 by Qiuxi Fan

ALL RIGHTS RESERVED

APPROVAL PAGE

IN VITRO DRUG DELIVERY BASED ON A POROUS MEMBRANE-BASED  
AQUEOUS-ORGANIC PARTITIONING SYSTEM AND ITS ENHANCEMENTS  
THROUGH MOUSE SKIN

Qiuxi Fan

11/30/04

---

Dr. Kamalesh K. Sirkar, Advisor  
Distinguished Professor of Chemical Engineering, NJIT  
Foundation Professor, Membrane Separations

Date

11/30/04

---

Dr. Bozena B. Michniak-Kohn, Co-advisor  
Associate Professor of Pharmacology and Physiology, UMDNJ

Date

11/30/04

---

Dr. Jing Wu, Co-advisor  
Assistant Professor of Chemical Engineering, NJIT

Date

11/30/04

---

Dr. Ken K. Chin, Committee Member  
Professor of Physics, NJIT  
Director of Materials Science and Engineering Program, NJIT

Date

11/30/04

---

Dr. David Kristol, Committee Member  
Professor of Biomedical Engineering, NJIT

Date

## BIOGRAPHICAL SKETCH

**Author:** Qiuxi Fan  
**Degree:** Doctor of Philosophy  
**Date:** January 2005

**Date of Birth:**

**Place of Birth:**

### **Undergraduate and Graduate Education:**

- Doctor of Philosophy in Materials Science and Engineering  
New Jersey Institute of Technology, Newark, NJ, 2005
- Master of Science in Mechanical Engineering  
Beijing Institute of Light Industry, Beijing, China, 1999

**Major:** Materials Science and Engineering

### **Presentations and Publications:**

- Qiuxi Fan, Kamalesh K. Sirkar, Yiping Wang, Bozena Michniak, 2004, "In Vitro Delivery of Doxycycline Hydrochloride Based on a Porous Membrane-based Aqueous-organic Partitioning System." *Journal of Controlled Release*. 98: 355-365.
- Qiuxi Fan, Kamalesh K. Sirkar, Bozena Michniak, 2004, "Iontophoretic Transdermal Drug Delivery System with a Conducting Polymeric Membrane." Submitted.
- Yiping Wang, Qiuxi Fan, Yifan Song, Bozena Michniak, 2003, "Effects of Fatty Acids and Iontophoresis on the Delivery of Midodrine Hydrochloride and the Structure of Human Skin." *Pharmaceutical Research*. 20:1612-1618.
- Yiping Wang, Rashmi Thakur, Qiuxi Fan, Bozena Michniak, 2004, "Transdermal Iontophoresis: Combination Strategies To Improve Transdermal Iontophoretic Drug Delivery." *European Journal of Pharmaceutics and Biopharmaceutics*. In press.
- Debabrata Bhaumick, Sudipto Majumdar, Qiuxi Fan, Kamalesh K. Sirkar, 2004, "Hollow Fiber Membrane Degassing in Ultrapure Water and Microbiocontamination." *Journal of Membrane Science*. 235: 31-41.



Qiuxi Fan, Kamalesh K. Sirkar, Yiping Wang, Bozena Michniak, 2004 In Vitro Delivery of Doxycycline Hydrochloride through Mouse Skin Based on an Aqueous-Organic Partitioning System, American Association of Pharmaceutical Scientists (AAPS) Annual Meeting, Baltimore, MD.

Qiuxi Fan, Kamalesh K. Sirkar, Yiping Wang, Bozena Michniak, 2004 In Vitro Transdermal Delivery of Doxycycline HCl Based on an Aqueous-Organic Partitioning System, NJCBM 7<sup>th</sup> Biomaterials Symposium, New Brunswick, NJ.

Yiping Wang, Qiuxi Fan, Yifan Song, Bozena Michniak, 2002 The Effect of Fatty Acids on the Iontophoretic Delivery of Lidocaine Hydrochloride, American Association of Pharmaceutical Scientists (AAPS) Annual Meeting, Toronto, Canada.

Yiping Wang, Qiuxi Fan, Yifan Song, Bozena Michniak, 2002 The Effect of Azone<sup>®</sup> on the Iontophoretic Delivery of Lidocaine Hydrochloride, American Association of Pharmaceutical Scientists (AAPS) Annual Meeting, Toronto, Canada.

To A. K. and C. P., for  
leading me through the troubled water

To my parents, for  
raising me up uninhibitedly in an inhibitive environment

赠予我的父母: 范铭华, 蒋佩珍,  
感谢你们的养育之恩: 给予我一个无拘无束的成长  
环境, 认识我自己, 成为我自己

## ACKNOWLEDGMENTS

I am truly grateful to my advisor, Dr. Kamallesh K. Sirkar. It is his patient mentoring and continuing challenges that have facilitated my transition from a “rookie” researcher.

Dr. Bozena Michniak, my co-advisor, has led me into the world of transdermal drug delivery (TDD) in academic field as well as in industrial applications. Most of the diffusion experiments were done in her distinguished Lab for Drug Delivery. She has also recommended me to practice my academic skills at Vyteris Inc., where I have learned to ask questions and solve them in the real world.

I am also thankful to Dr. Jing Wu, Dr. Ken Chin and Dr. David Kristol, who served in the committee and offered valuable comments and suggestions, to Dr. Ronald Kane, who provided financial support for my last year’s research, and to Dr. Marinos Xanthos, who made his laboratory available for polymer synthesis.

I am lucky to have worked with a group of talented and helpful people in both the Membrane Separations Lab and Drug Delivery Lab. Dr. Yiping Wang always voluntarily provided selfless assistance to me. I am indebted to Dr. Gordana Obuskovic, who would help me whenever I needed any help. Thanks also go to Dr. Baoan Li, whose rich experiences easily solved many of my difficulties; and Dr. Mohammad Al-Khalili, who answered my numerous questions about TDD.

My gratitude also goes to Dr. Jan Opyrchal, who kept on encouraging me from his own life experiences and all other friends, who trusted me and kept pushing me to a higher level.

## TABLE OF CONTENTS

Chapter	Page
1 INTRODUCTION.....	1
1.1 Background: Porous Membrane-Based Aqueous-Organic Partitioning System.	1
1.2 Does it Work in Transdermal Drug Delivery (TDD) Area?.....	4
1.3 Enhancements to Improve Drug Delivery through a Skin .....	7
1.3.1 Chemical Enhancements .....	8
1.3.2 Iontophoresis as a Means of Physical Enhancement .....	8
1.4 Application with Porous Conductive Membrane .....	12
1.5 Application with Porous Thermo-Sensitive Membrane .....	14
2 EXPERIMENTAL PROCEDURES .....	17
2.1 Types of Experiments .....	17
2.1.1 <i>In Vitro</i> Delivery Based on Aqueous-Organic Partitioning System through a Porous Polymeric Membrane Alone .....	17
2.1.2 <i>In Vitro</i> Delivery Based on Aqueous-Organic Partitioning System through Skin Membrane Alone .....	18
2.1.3 <i>In Vitro</i> Delivery Based on Aqueous-Organic Partitioning System through a Composite of a Porous Polymeric and a Skin Membrane .....	18
2.1.4 Enhanced <i>In Vitro</i> Delivery Based on Aqueous-Organic Partitioning System through a Composite of a Porous Polymeric and a Skin Membrane .....	18
2.2 Chemicals, Membranes (Polymeric and Skin Ones), Diffusion Cells and Patch	19
2.2.1 Chemicals .....	19
2.2.2 Membranes .....	20
2.2.3 Diffusion Cells .....	21

**TABLE OF CONTENTS**  
(Continued)

<b>Chapter</b>	<b>Page</b>
2.2.4 Patch .....	21
2.3 Preparation of Agent Solutions .....	22
2.3.1 Agent in Organic Solvents .....	22
2.3.2 Agent in Aqueous Solution .....	23
2.4 Preparation of Membranes .....	23
2.4.1 Preparation of Celgard® and PVDF Membranes .....	23
2.4.2 Preparation of PANi Membrane and its Properties .....	24
2.4.3 Preparation of Thermo-Sensitive PVDF Membrane .....	25
2.4.4 Preparation of Mouse Skin Membrane .....	25
2.5 Experimental Setup .....	25
2.6 Distribution Coefficient Study .....	27
2.7 LCST Study of Thermo-Sensitive Gel .....	28
2.8 SEM Imaging .....	28
2.9 HPLC Calibrations for Model Drugs Used .....	28
2.9.1 Doxycycline HCl and Lidocaine HCl .....	28
2.9.2 Caffeine .....	30
2.9.3 Nicotine .....	31
2.10 Calculations for Membrane Permeability, Agent Flux and its Accumulation ..	32
<b>3 RESULTS AND DISCUSSION .....</b>	<b>34</b>
3.1 Experimental Results of <i>In Vitro</i> Delivery of Doxycycline HCl Based on a Porous Membrane-Based Aqueous-Organic Partitioning System .....	34

**TABLE OF CONTENTS**  
(Continued)

<b>Chapter</b>	<b>Page</b>
3.1.1 Distribution Coefficient .....	34
3.1.2 Release Profiles from Polymeric Membrane Using 1-Octanol and Light Mineral Oil as Vehicle .....	34
3.2 Experimental Results of <i>In Vitro</i> Drug Delivery Based on a Porous Membrane-Based Aqueous-Organic Partitioning System through Mouse Skin	45
3.2.1 Release Profile of Doxycycline HCl from Porous Polymeric Membrane and Mouse Skin Using 10% Ethanol in Light Mineral Oil as Vehicle in the Reservoir .....	45
3.2.2 Release Profiles of Caffeine and Nicotine from Porous Polymeric Membrane and Mouse Skin Using 1-Octanol and Light Mineral Oil as Vehicle Respectively in the Reservoir .....	49
3.3 Experimental Results of <i>In Vitro</i> Drug Delivery through Mouse Skin Using Conductive Membrane as an Electrode .....	51
3.3.1 Properties of PANi Membranes .....	52
3.3.2 Aqueous Solution System .....	53
3.3.3 Aqueous-Organic Partitioning System .....	70
3.4 Experimental Results of <i>In Vitro</i> Delivery of Doxycycline HCl Based on an Aqueous-Organic Partitioning System through a Porous Thermo-Sensitive Membrane and a Mouse Skin .....	72
3.4.1 LCSTs of Thermo-Sensitive Polymeric Gels .....	72
3.4.2 Release Profiles from Porous Thermo-Sensitive Membrane .....	72
3.4.3 Release Profiles from a Composite of Porous Thermo-Sensitive PVDF and Mouse Skin Membranes .....	78
4 CONCLUSIONS AND RECOMMENDATIONS FOR FUTURE STUDIES .....	82
4.1 <i>In Vitro</i> Drug Delivery Based on an Aqueous-Organic Partitioning System through a Composite of Porous Polymeric and Skin Membranes .....	82

**TABLE OF CONTENTS**  
**(Continued)**

<b>Chapter</b>	<b>Page</b>
4.2 <i>In Vitro</i> Iontophoretic Drug Delivery through a Conductive Membrane as an Electrode Placed on a Mouse Skin .....	83
4.3 <i>In Vitro</i> Drug Delivery through a Porous Thermo-Sensitive Membrane Placed on a Mouse Skin .....	84
4.4 Recommendations for Future Studies .....	85
APPENDIX STRUCTURE OF DOXYCYCLINE HCL.....	87
REFERENCES .....	88

## LIST OF TABLES

Table	Page
2.1	Characteristic Properties of Different Polymeric Membranes ..... 20
3.1	Permeation Data Using 1-Octanol as Vehicle for Different Diffusion Systems ..... 37
3.2	Comparison of Calculated Flux Values and Experimental Ones..... 41
3.3	Permeation Data Using Light Mineral Oil as Vehicle for Different Diffusion Systems..... 43
3.4	Permeation Data through Mouse Skin with and without PVDF Membrane ... 46
3.5	Permeation Data through PVDF Membrane and Mouse Skin with Different Amounts of Linoleic Acid and through a Human Cadaver Skin..... 47
3.6	Permeation Data of Small Polar Agents through PVDF Membrane and Mouse Skin without Any Enhancer ..... 51
3.7	The Value of PANi Membrane Parameter ( $\epsilon_m/\tau_m$ ) Calculated from Data of Different Fluxes for Caffeine..... 53
3.8	Permeation Data for Three Agents Released through PANi Membrane ..... 54
3.9	Comparison of Model Predictions and Experimental Flux Data for Three Agents, Caffeine, Lidocaine HCl and Doxycycline HCl..... 55
3.10	Permeation Data of Three Agents Released through a Composite of PANi and Mouse Skin Membranes ..... 61
3.11	Iontophoretic Permeation Data of Three Agents Released through PANi Film ..... 62
3.12	Comparison of Model Predictions and Experimental Iontophoretic Flux Data ..... 63
3.13	Iontophoretic Permeation Data of Lidocaine HCl Released through Mouse Skin with and without a PANi Membrane ( $i=0.2\text{mA}/\text{cm}^2$ ) ..... 65
3.14	Iontophoretic Permeation Data of Doxycycline HCl Released through Mouse Skin with and without a PANi Membrane ( $i=0.3\text{mA}/\text{cm}^2$ ) ..... 66



**LIST OF TABLES**  
**(Continued)**

<b>Table</b>	<b>Page</b>
3.15 Permeation Data of Doxycycline HCl Released through Different Thermo-Sensitive Membranes at Different Temperatures .....	75
3.16 Permeation Data of DoxyHCl through 2%AA-PVDF and Mouse Skin Membranes .....	78
3.17 Permeation Data of Caffeine through 2%AA-PVDF and Mouse Skin Membranes .....	80

## LIST OF FIGURES

Figure	Page
1.1 The role of aqueous-organic partitioning on the diffusion through membrane pores filled with liquid (Farrell, 1996) .....	3
1.2 Schematic of skin structure (Adapted from Singh et al., 1994) .....	7
1.3 Schematic of principle of iontophoresis (Adapted from Burnette, 1989) .....	10
1.4 Schematic of an iontophoretic TDD system (Modified from Panchagnula et al., 2000).....	11
2.1 The two reservoirs-based controlled released cell (Farrell, 1996) .....	21
2.2 Schematic of Hill Top <sup>®</sup> patch .....	22
2.3 The iontophoretic setup using PANi film as a new electrode .....	27
2.4 Calibration curve for doxycycline HCl .....	29
2.5 Calibration curve for lidocaine HCl .....	30
2.6 Calibration curve for caffeine .....	31
2.7 Calibration curve for nicotine .....	32
3.1 Controlled release of doxycycline HCl through Celgard <sup>®</sup> 2400 membrane in the two reservoirs-based controlled release cell for the first five days (reservoir solvent, 1-octanol. Sol.2) .....	35
3.2 Controlled release of doxycycline HCl through Celgard <sup>®</sup> 2400 membrane in the two reservoirs-based controlled release cell for fourteen days (reservoir solvent, 1-octanol. Sol.2) .....	36
3.3 <i>In vitro</i> release of doxycycline HCl using 1-octanol as vehicle through PVDF or Celgard <sup>®</sup> 2400 membrane over 24 hr .....	37
3.4 <i>In vitro</i> release of doxycycline HCl using light mineral oil as vehicle through PVDF membrane over 24 hr .....	43
3.5 <i>In vitro</i> release of doxycycline HCl through mouse skin with and without PVDF membrane over 24 hr .....	45

**LIST OF FIGURES**  
(Continued)

<b>Figure</b>	<b>Page</b>
3.6 <i>In vitro</i> release profile of doxycycline HCl with linoleic acid as enhancer through PVDF membrane and mouse skin over 24 hr .....	47
3.7 <i>In vitro</i> release profile of doxycycline HCl with linoleic acid as enhancer through PVDF membrane and mouse skin over 120 hr .....	49
3.8 <i>In vitro</i> release profile of caffeine with 1-octanol as vehicle through PVDF membrane and mouse skin over 24 hr .....	50
3.9 <i>In vitro</i> release profile of nicotine with light mineral oil as vehicle through PVDF membrane and mouse skin over 24 hr .....	50
3.10 Release profiles of three agents through a composite of PANi and mouse skin membranes .....	61
3.11 Iontophoretic release profiles of lidocaine HCl through mouse skin with and without a PANi membrane ( $i=0.2\text{mA}/\text{cm}^2$ ) .....	64
3.12 Iontophoretic release profiles of doxycycline HCl through mouse skin with and without a PANi membrane ( $i=0.3\text{mA}/\text{cm}^2$ ) .....	66
3.13 SEM picture of doped PANi film used in the Ag AgCl set for doxycycline HCl diffusion .....	68
3.14 SEM picture of doped PANi film used in the Ag AgCl set for lidocaine HCl diffusion .....	69
3.15 SEM picture of doped PANi film used in the PANi AgCl set for doxycycline HCl diffusion .....	70
3.16 <i>In vitro</i> release of doxycycline HCl using light mineral oil as vehicle through PANi membrane over 6 hr .....	71
3.17 Schematic of PNIPAAm-co-AA synthesis .....	73
3.18 <i>In vitro</i> release of doxycycline HCl using light mineral oil as vehicle through PNIPAAm-PVDF membrane at two temperatures over 1 hr .....	74
3.19 <i>In vitro</i> release of doxycycline HCl using light mineral oil as vehicle through 2%AA-PVDF membrane at two temperatures over 1 hr .....	74

**LIST OF FIGURES**  
**(Continued)**

<b>Figure</b>	<b>Page</b>
3.20 SEM images of PVDF membrane surfaces with and without modification by thermo-sensitive gels .....	76
3.21 SEM images of PVDF membrane cross section with and without modification by thermo-sensitive gels .....	77
3.22 Thermo-sensitive permeation of doxycycline HCl through polymeric gel-immobilized PVDF membrane (Adapted from Park et al., 1998) .....	78
3.23 <i>In vitro</i> release of caffeine using 1-octanol as vehicle through 2%AA-PVDF membrane at two temperatures over 24 hr .....	80

## NOMENCLATURE

<i>A</i>	Diffusional area (cm <sup>2</sup> )
<i>C</i>	Agent concentration (μg/ml)
<i>D</i>	Diffusivity of the agent (cm <sup>2</sup> /sec)
<i>D<sub>eff</sub></i>	Effective diffusion coefficient of the agent in the pore (cm <sup>2</sup> /sec)
<i>D<sub>water</sub></i>	Diffusion coefficient of the agent in free solution (cm <sup>2</sup> /sec)
<i>D<sub>H<sub>2</sub>O</sub></i>	Diffusion coefficient of the agent in free solution (cm <sup>2</sup> /sec)
<i>F</i>	Faraday's constant (c/mol)
<i>i</i>	Current density (mA/cm <sup>2</sup> )
<i>J</i>	Permeate flux (μg/cm <sup>2</sup> -hr)
<i>k</i>	Mass transfer coefficient (cm/sec)
<i>K</i>	Distribution coefficient
<i>K<sub>1</sub></i>	First dissociation equilibrium constant
<i>K<sub>d</sub></i>	Dissociation equilibrium constant of dimer
<i>l</i>	Membrane thickness (mm)
<i>M</i>	Molecular weight (Da)
<i>P</i>	Permeability (cm/hr)
<i>Q</i>	Receptor accumulation after certain time (μg/cm <sup>2</sup> )
<i>Sh</i>	Sherwood number (kd <sub>i</sub> /D <sub>0</sub> )
<i>t</i>	Time (hr)
<i>t<sub>i</sub></i>	Transport number of ionic species <i>i</i>
<i>T</i>	Temperature (K)

$W$	Weight
$V$	Volume
$V_{caffeine}$	The molar volume of caffeine defined by Equation (3.12)
$z$	Charge value
$Z_i$	Electrochemical valence of the ion $i$

### Greek letters

$\rho$	Density
$\epsilon_m$	Membrane porosity
$\Delta$	Difference of the specific amount in the given time
$\tau_m$	Membrane tortuosity
$\eta$	viscosity (cP)
$\phi$	Association factor of solvent, dimensionless; for water: 2.6

### Subscripts

1	First
1D	Pore liquid of the donor side
1R	Pore liquid of the receptor side
di	Dimer
i	Species $i$
m	Membrane
m	Monomer as the subscript of $C$
T	Total

# CHAPTER 1

## INTRODUCTION

### **1.1 Background: Porous Membrane-Based Aqueous-Organic Partitioning System**

Membrane-based reservoir systems for controlled release have been extensively studied for a wide range of therapeutic applications, from oral formulations, transdermal patches to implants (Borodkin et al., 1975; Chien, 1982; Langer, 1990). Such a membrane system usually contains a reservoir for the agent sealed by a rate controlling polymeric membrane/film (Kydonieus, 1980). The diffusion of agent is first through the membrane then entering the targeted site. The first patent about a microporous membrane-bound reservoir device was obtained by Zaffaroni (Zaffaroni, 1976a), in which a gel, liquid or sol agent carrier with a limited solubility of the agent for release is utilized in the reservoir. A membrane wall, either porous or nonporous, is sealed beneath the reservoir; the membrane permeability is lower than that in the reservoir so that the ratio of the agent release rate through the reservoir to that through the membrane can vary based on different liquids in the reservoir and the pore (for porous membranes). However, the membrane properties (porosity, tortuosity, thickness), the agent concentration and the transport through the pore phase are major factors controlling the release rate.

A novel membrane-based controlled release system using aqueous-organic partitioning was intensely studied by Farrell and Sirkar (Farrell et al., 1997, 1999, 2001). This new device employs the agent's partitioning between an aqueous solution and an organic solution as a rate-controlling mechanism. The system consists of a reservoir containing the agent in an organic solution surrounded by a microporous membrane/film

with pores filled with aqueous liquid, or vice versa, aqueous solution in reservoir while organic liquid fills the pores. The partitioning of the agent takes place between the organic solution and the aqueous one at the interface of the reservoir and the mouth of the membrane pore. Since partitioning has replaced diffusion as the driving force in a large part for this device, longer term release at a constant rate (zero order) can be fulfilled by using an agent solution of high concentration in the reservoir. If a suspension of the agent is used in the reservoir, an extended zero order release can also be achieved, which overcomes the problem of short period of constant release often achieved by two other more commonly used means of controlled release: injection and ingestion.

In Farrell and Sirkar's study (Farrell et al., 1997, 1999, 2001), the reservoir is filled with either a pure agent liquid or an agent liquid of high concentration in an organic solvent (for organic agents). Water or an aqueous solution with a lower solubility for an agent is filled in the membrane pores in order to possess a very high aqueous-organic partition coefficient. This configuration greatly decreases the agent concentration in the aqueous pore phase and therefore reduces the rate of agent release; therefore an extended delivery is achieved. In another case, if the reservoir is filled with the agent in a concentrated aqueous solution, and an immiscible organic solvent is in the pore, the reservoir contains either pure agent or a concentrated agent solution, and therefore aqueous-organic partitioning is employed to reduce drastically the agent driving force for diffusion cross the membrane. Again, extended release is achieved. Figure 1.1 illustrates such a device and the role of partition on the diffusion through the membrane (Farrell, 1996; Farrell et al., 1997).



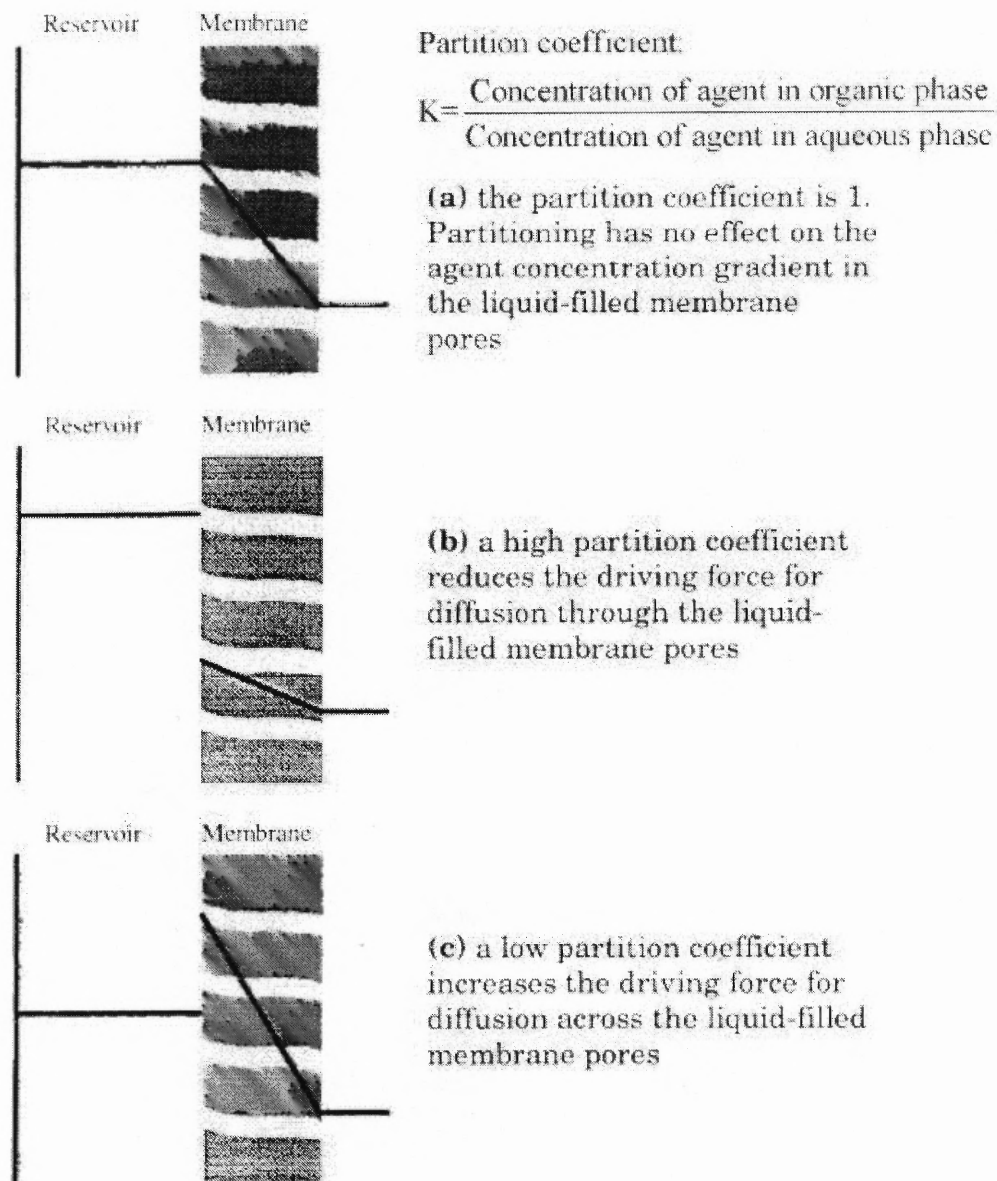


**Figure 1.1** The role of aqueous-organic partitioning on the diffusion through membrane pores filled with liquid (Farrell, 1996).

Scopolamine delivery system patented by Urquhart et al. (Urquhart, 1977, 1981) employ a mineral oil/polyisobutylene mixture with a very low solubility of agent scopolamine as the reservoir carrier and mineral oil filled in the pores of a microporous membrane. However, aqueous-organic partitioning is not applied. Several other

researchers also mentioned the existence of partitioning in nonporous membrane systems (Flynn et al., 1972; Theeuwes et al., 1976; Zaffaroni, 1976b, 1976a; Urquhart, 1977, 1981); however, it is Farrell and Sirkar who concentrated on demonstrating aqueous-organic partitioning as a means to control the release of agent from the system. This type of device can be used as a patch, stick-on, or an implant for drugs, fragrances, etc. without the complications of conventional devices such as drug stability during loading in a polymer, solvent processing in wet phase inversion, changing the polymer to certain shapes, etc. Such a system would achieve great flexibility in the release rate of the agent with the enormously different selections of the solute/solvent/membrane configuration.

### **1.2 Does It Work in Transdermal Drug Delivery (TDD) Area?**

Farrell and Sirkar's study showed the feasibility and potential for polymeric microporous membrane-based aqueous-organic partitioning system as controlled release devices, and also presented fundamental information on the release rates of the agent (Farrell, 1996). They investigated the release of an agent in the reservoir as a pure liquid using toluene diffusing across water-filled pores as well as agent partitioning in two cases: between an organic reservoir solution and water-filled pores and between an aqueous reservoir solution and organic-filled pores. The agent for the former system was benzoic acid, and the reservoir solvents were decanol and octanol; while for the latter one, aqueous nicotine was in the reservoir and pores were filled with mineral oil. They also studied the case of suspension in the reservoir and simultaneous release of two agents using caffeine and nicotine (Farrell et al., 1997, 2001). Their results showed that partitioning-controlled release system using a suspension in the reservoir can be fulfilled if the dissolution rate of

the agent into the reservoir is faster than that of transport through the membrane pores, and the aqueous-organic partition coefficient of an agent can be used to control its release rate from its concentrated solution of liquid in the reservoir. The time of extended release (zero-order) is a function of both the partition coefficient and the total amount of agent in the reservoir phase. The rate of the release is also affected by the physical characteristics of the microporous membrane. Farrell and Sirkar concluded that “when the aqueous-organic partition coefficient and the total amount of agent in the reservoir are large, partitioning will hardly affect the concentration in the reservoir, the reservoir will serve as an ‘infinite reservoir’ for the agent for an extended period of time, the agent’s concentration at the aqueous/organic interface at the pore mouth will remain essentially constant, and zero-order release will be achieved for a period of time.” (Farrell et al., 1997) They also indicated that “the duration of zero-order release was extended by the introduction of a suspension into the reservoir. If dissolution into the solvent is fast relative to diffusion out of the reservoir, zero-order release is extended due to the unchanging reservoir concentration.” (Farrell et al., 1997) Based on their experimental results and theoretical justifications, it seems that aqueous-organic partitioning-based controlled release system would satisfy the demand of delivering an agent constantly as long as necessary. Therefore, it is the rationale of further work based on this system in this dissertation.

Farrell and Sirkar’s work focused on some small molecules e.g., benzoic acid (MW: 122), nicotine (MW: 162) and caffeine (MW: 194), releasing from different polymeric microporous membrane based on aqueous-organic partitioning system. Will the transport of these smaller molecules through a composite of polymeric and skin

membranes be high enough to match the dose requirement of a particular disease? In addition, molecules of considerable interest are often larger, more complex and frequently polar, and therefore difficult to transport through the skin. It is certainly true of the broad-spectrum antibiotic, doxycycline hydrochloride (HCl) of molecular weight 480.1, which is licensed for the prophylaxis and treatment of malaria, acne and Reiter syndrome (Perkins et al., 1999). It would be of considerable interest to explore whether the reservoir-based technique based on the relatively simple aqueous-organic partitioning through a porous membrane could be employed in a skin patch to deliver important antibiotics e.g., doxycycline HCl, the molecular weight of which is almost 500; such a high molecular weight (MW) was considered for quite some time to be an upper limit for transdermal drug delivery (Bos et al., 2000). In this context, transdermal drug delivery of doxycycline HCl using aqueous-organic partitioning is considered demanding. Such a goal has been explored in a stepwise fashion first to examine whether this polymeric porous membrane-based aqueous-organic partitioning system works in transdermal drug delivery (TDD) area.

Transdermal drug delivery has been investigated around the world for several decades. Many drugs such as scopolamine, nitroglycerin, estradiol etc. have been successfully administered by TDD system. Compared with other drug administrations, TDD provides rapid onset and relative reliability. Sustained and constant plasma level can be achieved without generating patient discomfort (Chong et al., 1989).

For skin membrane, the fundamental part of TDD, there are three layers: epidermis, dermis, and subcutaneous as shown in Figure 1.2 (Singh et al., 1994). The uppermost layer of the epidermis i.e., the stratum corneum (SC) is the toughest barrier for

drug delivery because of its rigid, brick-shaped structure. For an agent like doxycycline HCl having a MW of almost 500 D to go through the skin, the need for a certain amount of enhancement to improve its delivery is obvious.

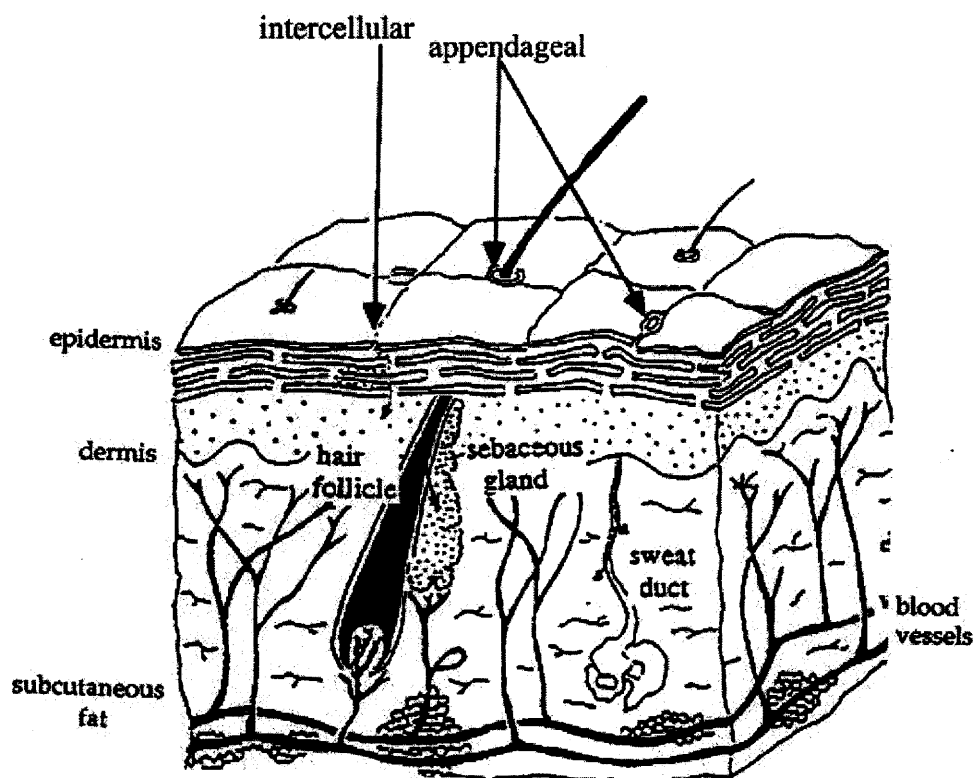


Figure 1.2 Schematic of skin structure (Adapted from Singh et al., 1994).

### 1.3 Enhancements to Improve Drug Delivery through a Skin

The enhancement for TDD is to employ an innocuous physical or chemical means to (Smith et al., 1995) increase the solubility of the drug in SC reversibly in order to facilitate diffusion of the agent through the barrier layer i.e., SC to the vasculature (Smith et al., 1995). Both chemical and physical enhancement have been tried to facilitate the transportation of the agent through skin.

### **1.3.1 Chemical Enhancements**

For chemical enhancements, the basic requirements of their properties are (Smith et al., 1995):

1. It should be specific without a pharmacological action of its own;
2. It should act promptly with a predictable duration and reversible effect;
3. It should be compatible with the agent and other components in the formulation and be chemically and physically stable;
4. It should be colorless, odorless, tasteless and nontoxic, nonallergenic, nonirritant.

Amide, terpene, fatty acids, etc. are mostly used chemical enhancers.

### **1.3.2 Iontophoresis as a Means of Physical Enhancement**

Iontophoresis, ultrasound, laser light, heat, etc. are generally used as physical enhancers. Among these, the iontophoretic technique, with its flexibility (different electrode materials, choices of current density, combination with other enhancements such as chemical enhancers, etc.) and outstanding releasing profile, has been the most investigated physical enhancement technique. In this dissertation work since the role of a polymeric membrane is focused on the TDD field as well, iontophoresis combined with a conducting polymeric membrane would not only be of great interest but could bring more options to the active TDD field.

The use of electrical current in drug delivery was first proposed in the middle of eighteenth century. The nineteenth century witnessed significant progress made by Hermann Munk, who first observed the systemic effects of iontophoresis in 1879, by Stephane Leduc, who first used iontophoretic technique, and by other scientists

(Helmstadter, 2001). The term “iontophoresis” is believed to have been introduced first by Fritz Frankenhauser (Helmstadter, 2001).

There are several advantages of iontophoretic TDD. First of all, it is a non-invasive way to deliver a drug into the body where great pain is eliminated without mechanical penetration (such as injections) and disruption of the skin. Another advantage is that drugs can be delivered either locally or systemically without potential systemic side effects. As the iontophoretic TDD is controlled by the current, the third advantage is that it can accurately control the timing of drug delivery (Rhodes III, 2002).

As a non-invasive TDD method, iontophoresis applies electrical current to deliver solubilized drugs through the skin to either the underlying tissue (local area) or capillaries and then to the whole circulating system (systemically). Two electrodes immersed in a drug solution and a voltage applied between the two electrodes have the drug (in the form of charged ions) moved from the donor part into the skin as shown in Figure 1.3 (Burnette, 1989). The positively charged electrode i.e., the anode, will attract the drug ions with negative charge, while the negatively charged electrode i.e., the cathode will attract the positively charged ions. Usually silver/silver chloride (Ag|AgCl) electrodes are used in such a system.

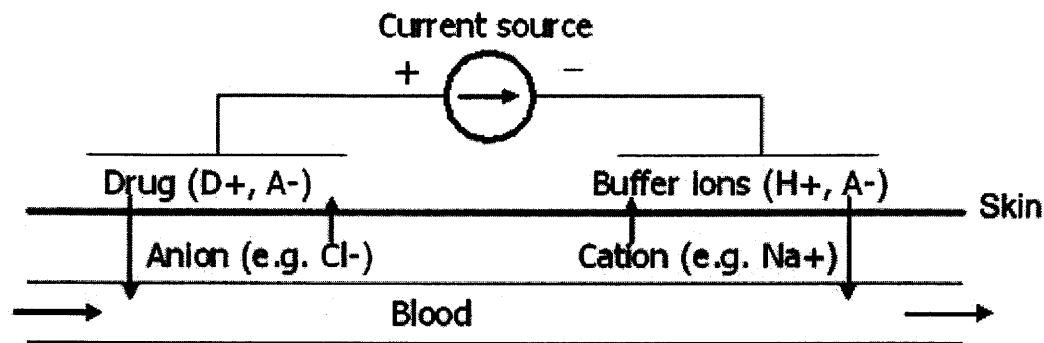


**Figure 1.3** Schematic of principle of iontophoresis (Adapted from Burnette, 1989).

For transdermal drug delivery, there are three general passive diffusion pathways for a drug going through the skin: transcellular, intercellular and transappendageal (Kanikkannan, 2002). The major route of iontophoresis transport is believed to be appendageal pores including the sweat ducts and hair follicles, which was proved by the investigations of several groups (Burnette, 1989; Singh et al., 1994; Kanikkannan, 2002). As to the pathway of the current facilitation, it is believed that the sweat ducts and glands are the major contributors (Grimnes, 1984), while for convective flow, hair follicles are the main pathway (Burnette, 1989; Singh et al., 1994; Kanikkannan, 2002). Figure 1.2 shows a schematic pathway of iontophoresis as well (Singh et al., 1994).

Figure 1.4 is a typical experimental setup for *in vitro* iontophoretic TDD study using side-by-side diffusion cell (Panchagnula et al., 2000).



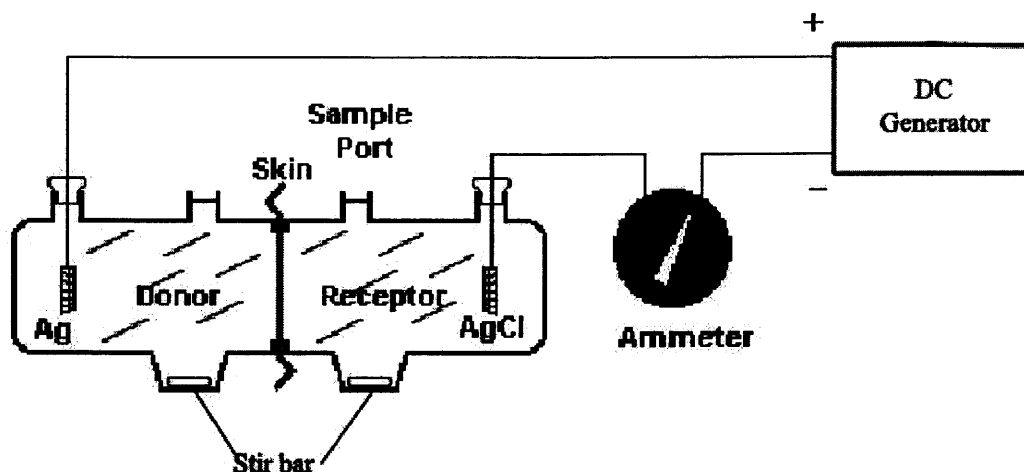


**Figure 1.4** Schematic of an iontophoretic TDD system (Modified from Panchagnula et al., 2000).

The system of Ag|AgCl electrodes are mostly used for iontophoretic study. Other materials such as sodium tungstate, graphite, transition metal dichalcogenide, prussian blue and polypyrrole could also be used as alternative electrodes (Banga, 1998). As desirable electrodes, they should possess good conductivity, flexible shape to match the skin surface, and most of all, minimal changes of pH (Panchagnula et al., 2000). Phipps' group studied platinum as anode and found the pH of donor solution changed from 5.9 to 2.6 resulting from the oxidation of water, while there was no such change for the Ag|AgCl set (Phipps et al., 1989).

However, not all agents are suitable for the application of iontophoretic TDD. Only water-soluble drugs of molecular weight under 10,000 ("10,000 Dalton Rule") are amenable to delivery (Wang et al., 2003). In addition, some patients may get redness, burning, and/or itching at the drug administration site. Besides, a stable power supply in a small size is also a big concern. Iontophoresis is still very promising for TDD. The first

pre-filled iontophoretic TDD patch for local anesthesia has been approved by FDA and will be available in the market soon (Kalia et al., 2004).

#### **1.4 Application with Porous Conductive Membrane**

As the transdermal delivery of doxycycline HCl through microporous polymeric and skin membranes via aqueous-organic partitioning would be investigated in the first part of this dissertation work, because of its relatively large MW, reduced accumulation was expected based on literature data (Perkins et al., 1999). On the other hand, the prophylactic oral dose of doxycycline is about 250 mg/week (MMWR, 1990). If 50% of it is bioavailable after the first-pass effect, around 18 mg should be transferred through skin in 24 h. Although the above TDD system could introduce the total amount required in 24 h using appropriate patch dimensions (Perkins et al., 1999), much faster delivery may be required for other drugs e.g., lidocaine hydrochloride (HCl). Iontophoresis as a means of facilitation to achieve fast delivery is investigated here to increase the accumulation using a novel conducting polymeric membrane as electrode.

As a conducting polymer, polyaniline (PANi) has attracted many researchers to explore its unique properties and then apply it into different fields. In the area of controlled release, its possibility to transform itself from almost an insulator to a high conductor in different pH environments is the focus. In other words, it could be a very good candidate membrane to carry out ion exchange, which matches the requirement of the iontophoretic technique.

Due to its good environmental stability, easy synthesis, and special electrical and mechanical properties, many researchers have concentrated on the permeability of PANi

membrane for gases, water and small carboxylic acids (Wen et al., 1999); however, no paper is available on iontophoretic TDD study, especially for large MW molecules such as lidocaine HCl, doxycycline HCl.

In the iontophoretic TDD area, PANi could be used as an electrode to bind agent ions illustrated in several patents (Parsi, 1988; Haak et al., 1990; Reynolds et al., 2002), as a conductive membrane to split the donor chamber (Sanderson et al., 1988; Phipps, 1991, 1992), or only as an anode electrode (Untereker et al., 1992; Scott, 2001; Siman et al., 2001; Fischer et al., 2004). However, none of them disclosed a doped PANi membrane which functions simultaneously as both an anode and a control membrane for the iontophoretic transdermal drug delivery system separating the donor reservoir from the receptor.

Therefore, it would be a useful development if one can employ the conducting polymer membrane film directly as an electrode in the iontophoretic technique, making it both a controlled release membrane and an electron carrier. Such a system may eliminate the unstable Ag part of traditional Ag|AgCl electrodes; at the same time a patch based on such a new system is reusable instead of replacing Ag|AgCl electrode. Not only the current density but also the membrane would control the release rate of drug: applying different pore sizes of such films and adjusting the current, different sizes of molecules from small (less than 200 D) to large (several thousand and larger) could go through, which makes it possible to deliver several agents at different rates in one system. Lastly, such a system is considerably cheaper than that of Ag|AgCl electrodes.

The objective in this second part of dissertation is first to synthesize the porous PANi membrane and then employ it in a specific iontophoretic TDD system to study the

permeation of different agents. Since it is a novel iontophoretic TDD using PANi membrane as electrode, agents having different MW ranging from 200D to 500D in their aqueous solutions would be primarily investigated. Next, aqueous-organic partitioning between the reservoir and the liquid in the membrane pore would be tested. The regular set of Ag|AgCl electrodes would also be used in conventional iontophoretic system to compare the permeation results with this new electrode system.

### **1.5 Application with Porous Thermo-Sensitive Membrane**

A further practical employment of the porous membrane-based aqueous-organic partitioning system on TDD area is to combine certain thermo-sensitive polymers into/onto the porous membrane system to form an “intelligent” TDD system. Fever, a body condition where its core temperature becomes higher than normal, is the symptom of many diseases (Vander et al., 1994) like malaria. When fever is detected, usually an antibiotic such as doxycycline HCl should be taken immediately to prevent the worsening of condition. The goal of this application is to coat a porous membrane or/and fill its pores with a thermo-sensitive polymeric gel, which has a responsive range of temperatures matching normal and fever temperatures of skin, then releases the antibiotic i.e., doxycycline HCl, only under fever conditions.

Since 1940s many papers have investigated comb-like polymers with long side-chains which can crystallize independent of the main-chain (Mogri et al., 2000). Such polymers may vary in their structures but have one common characteristic: they always possess long alkyl groups extending from the main-chain. The specific property of these polymers is that as their melting point is a critical structure transforming juncture, their

permeability can be changed dramatically because of different morphology around this temperature. That is: below the melting point of the side-chain crystals, the rigid but brittle nature of those semi-crystalline materials becomes effective permeation obstacle with the branch chain-based crystallinity; above such a point they appear softer like a fluid and have much higher permeability owing to their amorphous structure. This unique thermo-sensitive property has found polymers of this category applied to a wide range of areas such as medical, agrochemical and industrial areas in which temperature-controlled release is required. Examples of such applications are seed coating linking germination to soil temperature, pesticide optimum-timing release related to the certain temperature, and nitroglycerin transdermal release in a pulsatile way (Greene et al., 1993).

Among these “intelligent” polymers, poly-N-isopropylacrylamide (PNIPAAm) has been intensely studied. In an aqueous solution it has a lower critical solution temperature (LCST) of about 32°C (Yoshida et al., 1993; Vernon et al., 1996; Lin et al., 2003), which is around to normal skin temperature (Bronaugh et al., 1991). Its linear or branch form dissolves in water below the LCST and precipitates above it. If it is crosslinked, it forms a temperature-responsive hydrogel, which swells below and deswells above the LCST. Such reversible thermo-sensitive polymer or its gels have been applied in many biomedical fields: biosensing, immobilization of enzymes or bioactive materials, controlled drug release, protein purification and affinity separation, etc.

In the case of a TDD system, regulation of the drug delivery is achieved by turning “on” and “off” the rate controlling membrane in the transdermal device. This membrane is fabricated from a thermo-sensitive polymer that undergoes a reversible phase transition at a certain temperature (LCST). When the device is in contact with

warm skin, the membrane is below its LCST and is “crystalline”, therefore, impermeable. However, with an ailing body, in most cases the skin temperature rises a little so that the polymer membrane can be warmed above the LCST. Then it becomes amorphous and very permeable to deliver the drug into the blood through skin steadily and continuously until the disease is cured and the skin temperature is back to normal.

In order to make the LCST of PNIPAAm match the changes of physical temperature, there are several ways of achieving chemical modifications for tailoring it such as change of its hydrophilic/hydrophobic balance (Vernon et al., 1996), i.e., adding extra hydrophilic comonomer like acrylic acid (AA) (Lin et al., 2003); change of the block length of PNIPAAm (Mogri et al., 2001); adjustment of pH of polymer solution (Luyten et al., 1999), etc.. Among those studied, AA comonomer has been investigated most intensively and presented satisfactory results (Vernon et al., 1996; Lin et al., 2003).

To sum up, the relatively large molecule, doxycycline HCl is the basic model drug to be tested for *in vitro* transdermal delivery based on the porous membrane based aqueous-organic partitioning system. Several polymeric porous flat membranes, i.e., hydrophobic Celgard<sup>®</sup> (polypropylene) and hydrophilic PVDF (polyvinylidene fluoride), PANi film and PVDF coated with thermo-sensitive gel would be tested first to examine whether the polymeric membrane would be a major obstacle for the agent to go through. Then a skin membrane would be added beneath the polymeric one to test the percutaneous diffusion performance. Since the present dissertation work was an initial feasibility study for such a configuration, mouse skin was used in all *in vitro* experiments.

## CHAPTER 2

### EXPERIMENTAL PROCEDURES

#### 2.1 Types of Experiments

Three types of membrane configurations were used in this dissertation: polymeric membrane; skin membrane; a composite of polymeric and skin membranes. Four types of *in vitro* membrane permeation experiments were implemented: polymeric membrane alone, skin membrane alone, a composite of polymeric and skin membranes and such a composite with enhancement.

##### **2.1.1 *In Vitro* Delivery Based on Aqueous-Organic Partitioning System through a Porous Polymeric Membrane Alone**

This type of experiment was used to examine whether the porous polymeric membrane would be a major obstacle for a relatively large and polar drug molecule (agent) i.e., doxycycline HCl (MW: 480.1) to go through with aqueous-organic partitioning taking place along the diffusion path. Two types of polymeric membranes were tested: hydrophobic and hydrophilic membranes using a couple of agent solutions having different concentrations in the donor solutions prepared from a number of organic liquids as solvents. As an extension of the study by Farrell and Sirkar (Farrell, 1996; Farrell et al., 1997, 1999, 2001), a two reservoirs-based controlled release cell (Farrell, 1996) was also used in this type of permeation tests along with the regular Franz diffusion cells. A patch system using the same membranes was then tested employing the Franz cell.

In the controlled release application using a porous conductive membrane, because of its novelty, a fundamental study of delivering agents of different MWs from

their aqueous solutions was of primary focus.

### **2.1.2 *In Vitro* Delivery Based on Aqueous-Organic Partitioning System through Skin Membrane Alone**

The results from a porous membrane-alone type of permeation experiments facilitated the selection of the polymeric membrane, concentration of agent solution and the solvent. Franz cell was used for all permeation experiments with the skin membrane only. The results from this type of experiment were used as control tests to compare the earlier results from those using polymeric membrane alone and using a composite of polymeric and skin membranes.

### **2.1.3 *In Vitro* Delivery Based on Aqueous-Organic Partitioning System through a Composite of a Porous Polymeric and a Skin Membrane**

The results from this type of experiments provided a perspective of TDD based on aqueous-organic partitioning system through a composite of a porous polymeric and a skin membrane: whether there was decent release from this system, whether the accumulation was too low or even zero, and whether enhancements should be used to facilitate agent transport for the next type of experiments.

As for the application with porous conductive membrane, agent in its aqueous solution ended up being the primary focus.

### **2.1.4 Enhanced *In Vitro* Delivery Based on Aqueous-Organic Partitioning System through a Composite of a Porous Polymeric and a Skin Membrane**

Except for the application with a porous conductive membrane, chemical enhancements were employed for the delivery of doxycycline HCl. Enhancers from three widely used categories, amide, terpene and fatty acid (Smith et al., 1995), were tested to search for a



specific compound which worked. Different enhancer concentrations were investigated.

As for the application with a porous conductive membrane, since iontophoresis itself is a means of enhancing transport, no chemical enhancer was employed unless no release was detected by iontophoresis. The first set of tests employed the agent in its aqueous solution. Then TDD based on aqueous-organic partitioning system was tested.

## **2.2 Chemicals, Membranes (Polymeric and Skin Ones), Diffusion Cells and Patch**

### **2.2.1 Chemicals**

Doxycycline HCl (MW: 480.1), Sigma brand, was donated by Integrated Pharmaceuticals, Boston, MA. Lidocaine HCl (MW: 270.8) was purchased from Aldrich, Milwaukee, WI. Caffeine (MW: 194.2) and nicotine (MW: 162) were purchased from Fisher Scientific, Fair Lawn, NJ.

Potassium phosphate monobasic anhydrous, acetic acid, azone, cineole and linoleic acid were obtained from Sigma (St. Louis, MO). Light mineral oil, 1-octanol, glycerol, ethanol, methanol (HPLC-grade) and acetonitrile (HPLC-grade) were purchased from Fisher Scientific, Fair Lawn, NJ. Phosphate buffered saline (PBS) was supplied by Fluka, Milwaukee, WI. Bio-PSA<sup>®</sup> 7-4302 silicone adhesive was from Dow Corning Corp., Midland, MI.

Silver wire (99.9%, 0.5mm), silver chloride (99.9%), hydrochloric acid solution (1N) and NMP were purchased from Fisher Scientific (Fair Lawn, NJ).

Polyaniline (emeraldine base, MW ca. 65,000), N-isopropylacrylamide (NIPAAM), acrylic acid (99%) (AA), N, N-methylene bisacrylamide (99%) (BIS), N, N, N', N'-tetramethylene diamine (TEMED) and ammonium persulfate (APS) were

purchased from Sigma-Aldrich, Milwaukee, WI.

### 2.2.2 Membranes

Celgard<sup>®</sup> 2400 hydrophobic polypropylene flat films were from Celgard (Charlotte, NC). Polyvinylidene fluoride (PVDF) Durapore<sup>®</sup> hydrophilized films were purchased from Millipore Corp. (Bedford, MA). The polymer PVDF is naturally hydrophobic; an additional polymerized layer on the membrane surface and pores makes it hydrophilic. Table 2.1 provides details of the polymeric membrane properties and dimensions.

**Table 2.1** Characteristic Properties of Different Polymeric Membranes

Microporous membrane	Material	Pore size (μm)	Porosity <sup>a</sup>	Tortuosity	Membrane thickness (μm)
Celgard <sup>®</sup> 2400 film	Polypropylene	0.035×0.2	0.38	5.0 <sup>b</sup>	25
PVDF film	Polyvinylidene fluoride	0.1	0.7	2.58 <sup>c</sup>	100

<sup>a</sup>Supplied by manufacturer.

<sup>b</sup>Prasad et al., 1988.

<sup>c</sup>Chen et al., 1999.

Polyaniline membrane was cast by evaporating polyaniline (emeraldine base) (PANi) solution in NMP.

Thermo-sensitive gels, PNIPAAm and PNIPAAm-co-AA, were synthesized by radical polymerization.

Skin membranes: Male hairless mice, strain SkH1, 8 weeks old, were supplied by Charles River Laboratories (Wilmington, MA). Mice were euthanized by carbon dioxide asphyxiation. Their skins were excised and kept at -30°C until used.

### 2.2.3 Diffusion Cells

Two different diffusion cells were used. The first one consisted of two reservoirs-based controlled release cell, each reservoir having a volume of about 0.9 ml and a diffusional area of  $2.53 \text{ cm}^2$  (shown in Figure 2.1) (Farrell, 1996). The other one was a standard Franz diffusion cell (PermeGear, Inc., Bethlehem, PA), with a diffusional area of  $0.64 \text{ cm}^2$  and a receptor compartment volume of 5.1 ml; for the patch system, the values of the corresponding parameters were:  $3.14 \text{ cm}^2$  and 9.5 ml.

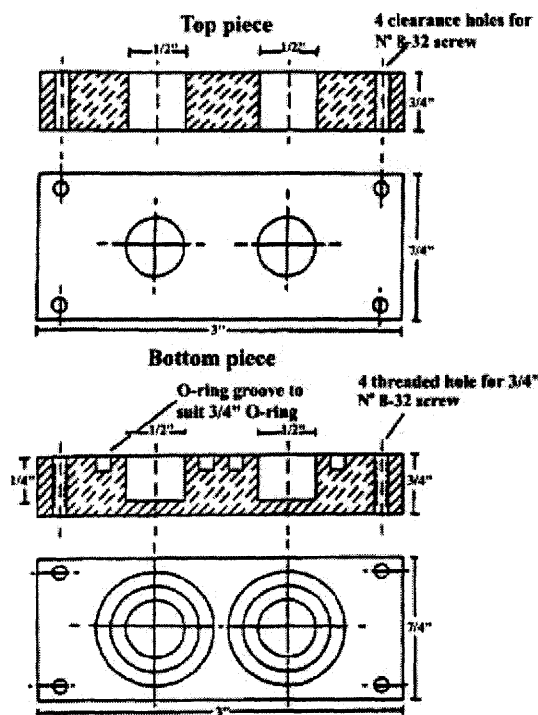
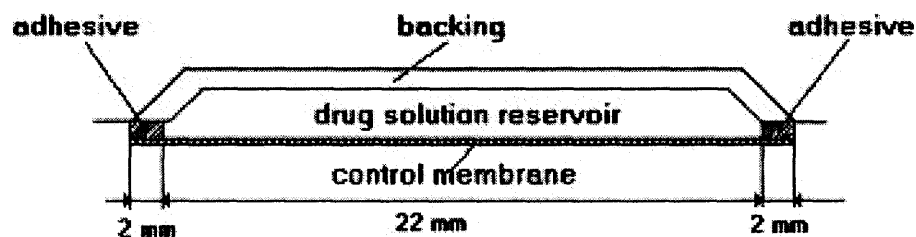


Figure 2.1 The two reservoirs-based controlled released cell (Farrell, 1996).

### 2.2.4 Patch

Patches used were supplied by Hill Top Research, Inc., Cincinnati, OH. Figure 2.2 is a schematic of the patch.



**Figure 2.2** Schematic of Hill Top<sup>®</sup> patch.

## 2.3 Preparation of Agent Solutions

### 2.3.1 Agent in Organic Solvents

For doxycycline HCl as the agent, with 1-octanol as solvent, either 250 mg (Sol.1) or 500 mg (Sol.2) of the agent was transferred into 50 ml of 1-octanol. Then the solution was stirred for 12 hours till it became clear for use. For light mineral oil as solvent, the agent had a much lower solubility than that in 1-octanol. The amount added was 500 mg into 50 ml of light mineral oil so that there was enough agent present in a suspension. In another case, the agent sample (500 mg) was suspended into 50 ml of 10% v/v ethanol in light mineral oil and agitated over a magnetic stirrer for 12 hours. Fifteen minutes before applying the agent solution into the donor part of the diffusion cells, certain amount (5, 10, 20% v/v) of enhancer (azone, cineole, or linoleic acid) was sometimes added into the solution as a suspension and thoroughly mixed. For the 1-octanol-based systems, no ethanol or enhancer was applied.

For caffeine as the agent, an amount of 200 mg of the agent was transferred into 20 ml 1-octanol. Then the suspension was stirred for 12 hours before use.

For nicotine as the agent, an amount of 0.2 ml of the agent was transferred into 20 ml light mineral oil. Then the solution was stirred before use.

### **2.3.2 Agent in Aqueous Solution**

Solutions of caffeine and doxycycline HCl in water were prepared by dissolving about 200 mg of each agent into 10 ml of water, while about 400 mg of lidocaine HCl was dissolved into 10 ml of water. A solution of about 200 mg doxycycline HCl dissolved into 10 ml of an ethanol-water mixture (EtOH:H<sub>2</sub>O=2:1 v/v) with 5%v/v linoleic acid was also prepared.

## **2.4 Preparation of Membranes**

### **2.4.1 Preparation of Celgard<sup>®</sup> and PVDF Membranes**

A piece of Celgard<sup>®</sup> or PVDF film was cut into a circular shape having an area same as that of the diffusion cells. The Celgard<sup>®</sup> film was wetted by the following steps: the film was dipped in 40% v/v ethanol/DI water solution for 4 hours, then was transferred to 20% v/v ethanol/DI water solution overnight; after that the film was moved to 5% v/v ethanol/DI water solution overnight; the last step was to soak it in DI water overnight. Then these circular films were soaked into 10 % v/v ethanol/deionized water for 10 minutes; the water drops remaining on both surfaces were removed by rolling a glass rod over the membrane. For the two reservoirs-based cells, the wetted membranes were placed over each reservoir, and the cells were closed.

### 2.4.2 Preparation of PANi Membrane and its Properties

For the preparation of a PANi film, an amount of 1.5 g of polyaniline was dissolved into 100 ml NMP and stirred for 1 hr (MacDiarmid et al., 1996). A regular gauze pad was used to filter the resulting dark blue solution. The clear filtrate solution was then transferred to a Rotavapor® RE 111 (Flawil, Switzerland) to evaporate the solvent at 50°C (MacDiarmid et al., 1996) for about 70 minutes to yield about 20 ml of a sticky solution. The PANi film was cast from such a solution on a glass plate. Doping such a film was achieved by keeping the film in a solution of 1N HCl for 24 hr (MacDiarmid et al., 1996) then washing it by DI water and drying it.

The porosity of the membrane was obtained by measuring the weights of membrane wetted with glycerol and dry membrane, converting the difference into the void volume by taking the density of glycerol into account and then dividing by the dry volume of the film. The Equation for the calculation of membrane porosity ( $\epsilon_m$ ) is:

$$\epsilon_m = \frac{(W_{wet} - W_{dry}) / \rho_{glycerol}}{V} \quad (2.1)$$

where,  $W_{wet}$  and  $W_{dry}$  are the weights of wet and dry membrane, respectively.  $\rho_{glycerol}$  (1.475 gm/ml) and  $V$  are the density of glycerol and the total volume of the membrane, respectively.

The calculation of the value of the membrane parameter ( $\epsilon_m/\tau_m$ ) was carried out by measuring the flux data from three diffusion experiments of caffeine with three different concentrations as all other conditions were kept the same.

### 2.4.3 Preparation of Thermo-Sensitive PVDF Membrane

Thermosensitive gels based on PNIPAAm and PNIPAAm-*co*-2%AA, were synthesized by radical crosslinking copolymerization in aqueous solution: first an amount of 10 gms NIPAAm, 0.5 mol% BIS, 1 mol% APS were transferred into 190 ml water with or without 2 mol% AA. After bubbling with nitrogen for 10 minutes in a water/ice bath (Huglin et al., 1997), 1 mol% TEMED was added into the solution along with 20 small pieces of PVDF membranes. Then the system was left to polymerize in a water bath at room temperature for 6 hr (Huglin et al., 1997). Before the diffusion experiments, coated/soaked PVDF membranes were carefully pulled out from the gel solutions and the gel attached on both surfaces of membrane were removed.

### 2.4.4 Preparation of Mouse Skin Membrane

The mice skins were first taken out from the freezer (-30°C) and put into a beaker filled with room temperature water until they were defrosted. The mice skins from their dorsal (back) sites were removed from the adhering fat deposits and then were cut into small pieces of appropriate size and carefully mounted on top of the diffusion cells and left to hydrate. After 1 hour of hydration, a drop of either 1-octanol or light mineral oil (depending on which organic solvent was used) was applied on the surface of each piece of mouse skin to wet it for 10 minutes if agent used was in organic solvent. Then each piece of skin was covered carefully with the circular polymer membrane piece.

## 2.5 Experimental Setup

The donor part of the Franz diffusion cell was filled with 0.5 ml of the suspension (if there was a suspension as in light mineral oil) containing agent solution, and the receptor

compartment with isotonic phosphate buffer (pH 7.2) containing 0.1% v/v of 36% aqueous formaldehyde as preservative (Sloan et al., 1991). Receptor solution temperature was maintained at  $37 \pm 0.5^\circ\text{C}$  and was constantly stirred at 600 rpm. The top of the donor compartment was covered with triple layers of Parafilm<sup>®</sup>. At predetermined times, 300  $\mu\text{l}$  samples were taken from the receptor compartment over a total period of either 24 or 120 h and were immediately replaced by the same volume of a fresh buffer solution. The samples were kept frozen at  $4^\circ\text{C}$  prior to analysis by high performance liquid chromatography (HPLC). The results are based on averages from 3 Franz cells.

The amount of the agent withdrawn with a sample was corrected in the subsequent calculation of the cumulative amount penetrated. For the two-reservoirs-based-cell, after preparation of the flat membrane system, the device was submerged in a volume of water chosen for analytical convenience, between 150 – 750  $\text{cm}^3$ . Samples having a volume of 200  $\mu\text{l}$  were withdrawn periodically from the aqueous phase in the glass vessel until agent concentration remained constant for three consecutive measurements. The sample volume was negligible compared with the total aqueous volume and the agent concentration in the surrounding water was extremely low relative to its saturation concentration; therefore medium changes were not necessary. The mass of agent released was calculated from the aqueous concentration and bath volume, and plotted as a function of time to establish release profiles.

For the experiments using PANi membranes, they were cut to the shape fitting the Franz diffusion cells. If delivery was facilitated by iontophoresis, such films were applied in a large enough size to have its edge extruding out so that it could be connected to the direct current (DC) power source as an anode (setup shown in Figure 2.3). The DC was



generated by the stimulus isolator purchased from World Precision Instrument, Inc., Sarasota, FL. The details of the preparation of Ag|AgCl electrodes is available elsewhere (Wang et al., 2003). All results are based on an average of the data from three Franz cells.

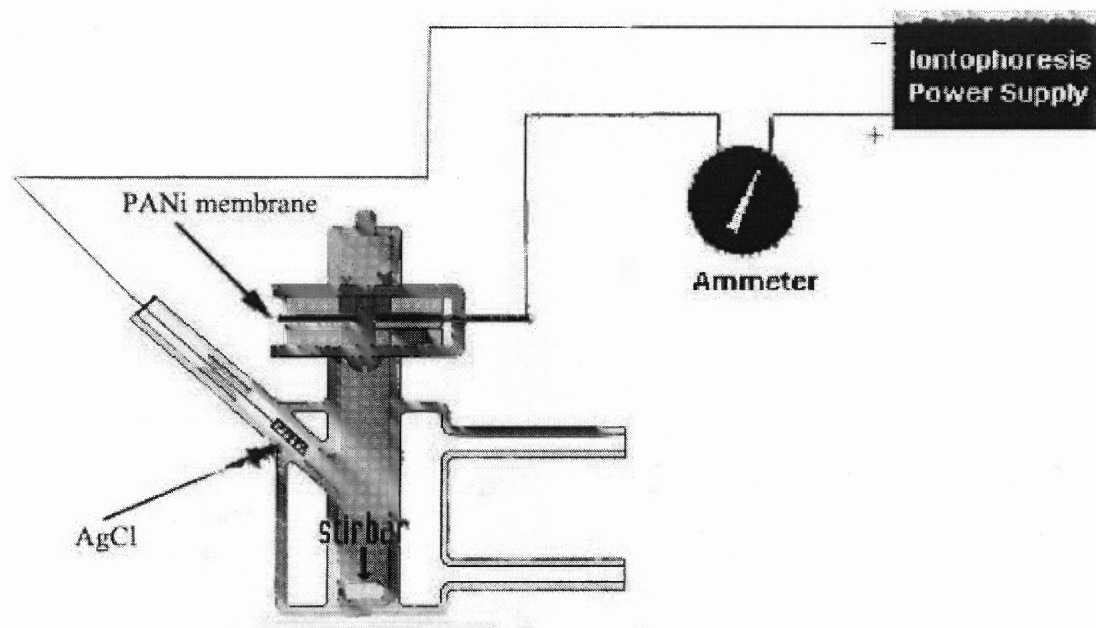


**Figure 2.3** The iontophoretic setup using PANi film as a new electrode.

For the experiments using thermo-sensitive PVDF membranes, the water temperature of the circulating bath was adjusted so that the surface temperatures of the mouse skin would be either 32°C or 33°C, simulating the conditions of normal and fever body temperatures, respectively.

## 2.6 Distribution Coefficient Study

A certain amount of agent was transferred to different volumes of deionized water, respectively. Then the same volume of organic solvent e.g., 1-octanol or light mineral oil was added into the same container. Each container was put on the stir plate and stirred for

24 hours. The aqueous phase was centrifuged and its concentration of agent was analyzed by high performance liquid chromatography (HPLC) as described later.

## **2.7 LCST Study of Thermo-Sensitive Gel**

The measurements of the LCSTs of different thermo-sensitive gels were carried out in a DSC Q100 (TA Instruments, New Castle, DE). Sample weights were around 25 mg. Scanning temperatures were from 0°C to 50°C at a scanning rate of 5°C/min.

## **2.8 SEM Imaging**

Membrane structure was characterized using a scanning electron microscope (SEM) (LEO 1530 VP FE-SEM, Carl Zeiss, New York, US).

## **2.9 HPLC Calibrations for Model Drugs Used**

### **2.9.1 Doxycycline HCl and Lidocaine HCl**

Samples containing doxycycline HCl were analyzed by reverse phase high performance liquid chromatography (HPLC), using a 4.6 × 150 mm Phenomenex Luna C18 5 μm ODS column fitted to a Hewlett Packard 1090 automated isocratic system, with UV detection at 346 nm (Perkins et al., 1999). The mobile phase consisted of 45:55 (v/v) of acetonitrile and 0.02 M KH<sub>2</sub>PO<sub>4</sub> in deionized water. The pH of this salt eluent was adjusted to 3.0. Before use, the solution was degassed and filtered through Nalgene™ 0.2 μm nylon filter (Nalge Company, Rochester, NY). The injection volume was 40 μl and the flow rate was set at 1.0 ml min<sup>-1</sup>. Under these conditions, a retention time of

approximately 2 min was obtained for the agent. A calibration plot for doxycycline HCl is shown in Figure 2.4. The equation of the regression line is:  $y=57871x-255488$ .

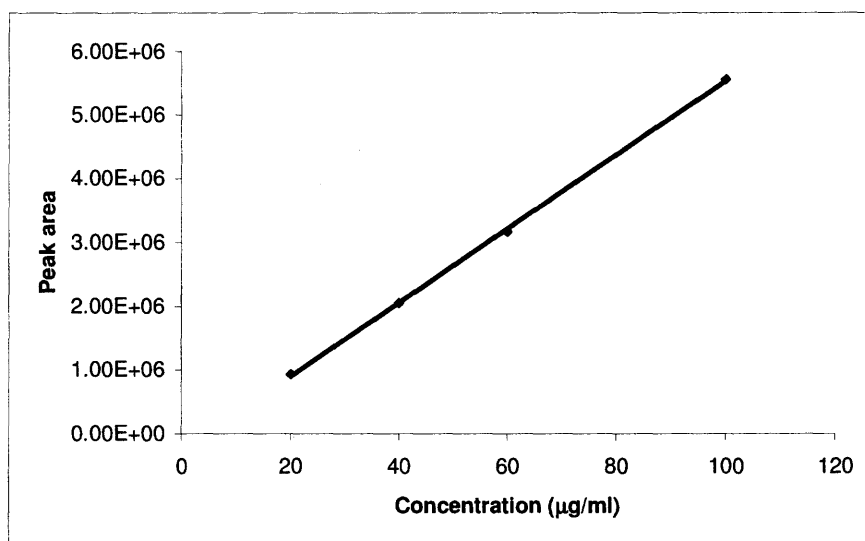


**Figure 2.4** Calibration curve for doxycycline HCl.

For lidocaine HCl, HPLC analysis was performed using a Hewlett Packard 1100 LC with a reverse-phase  $C_{18}$  column (Microsorb-MV<sup>TM</sup>, 15 cm, 5 µm, Agilent Technologies) at a flow rate of 1 ml/min. Samples were detected at 220 nm using a mobile phase having the composition of acetonitrile: 0.05 M monobasic potassium phosphate (45:55 v/v, pH 3.0) and an injection volume of 40 µl. A calibration plot for lidocaine HCl is shown in Figure 2.5. The equation of the regression line is:  $y=56x+129$ .

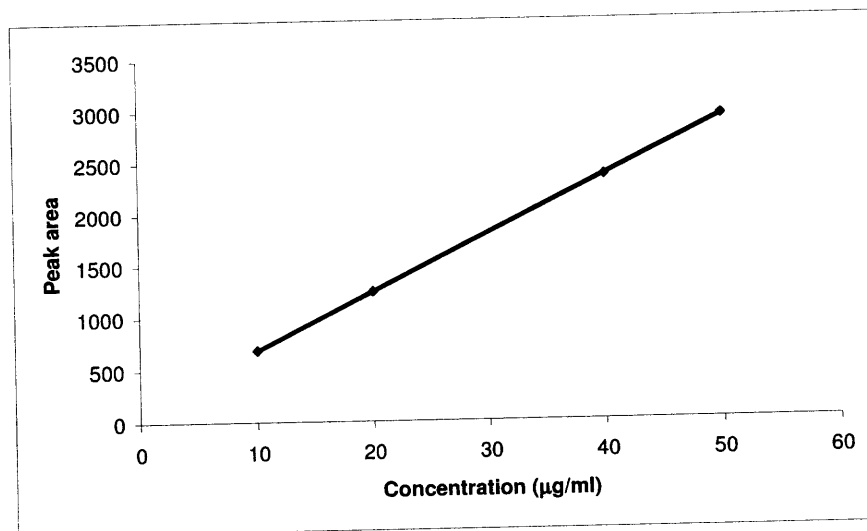


**Figure 2.5** Calibration curve for lidocaine HCl.

### 2.9.2 Caffeine

For caffeine, HPLC analysis was performed using a Hewlett Packard 1100 LC with a reverse-phase  $C_{18}$  column (Microsorb-MV<sup>TM</sup>, 15 cm, 5  $\mu$ m, Agilent Technologies) at a flow rate of 1 ml/min. It was detected at 270 nm using a mobile phase composition of acetonitrile: methanol: water (10:20:70 v/v/v) and an injection volume of 20  $\mu$ l. A calibration plot for caffeine is shown in Figure 2.6. The equation of the regression line is:  $y=64x-86$ .

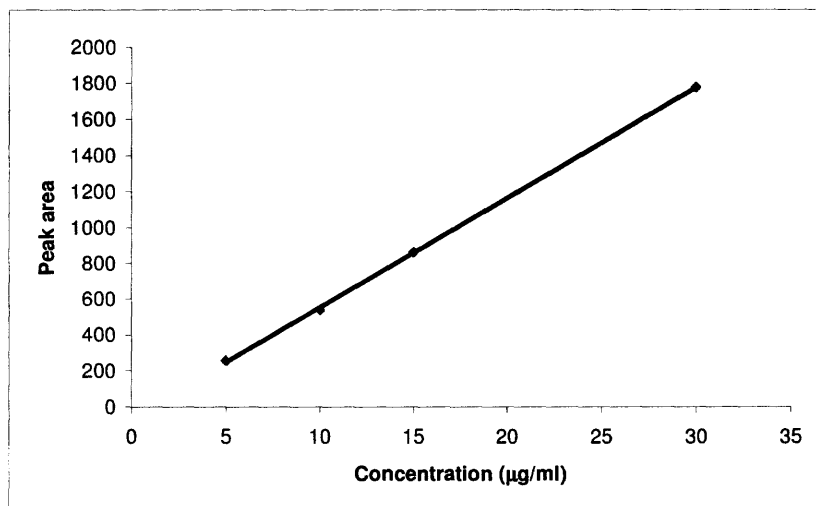


**Figure 2.6** Calibration curve for caffeine.

### 2.9.3 Nicotine

For nicotine, HPLC analysis was performed using a Hewlett Packard 1100 LC with a reverse-phase  $C_{18}$  column (Microsorb-MV<sup>TM</sup>, 15 cm, 5 µm, Agilent Technologies) at a flow rate of 1 ml/min. It was detected at 254 nm using a mobile phase composition of methanol: water: acetic acid (45:55:1 v/v/v) and an injection volume of 50 µl. A calibration plot for nicotine is shown in Figure 2.7. The equation of the regression line is:  $y=11x+17$ .

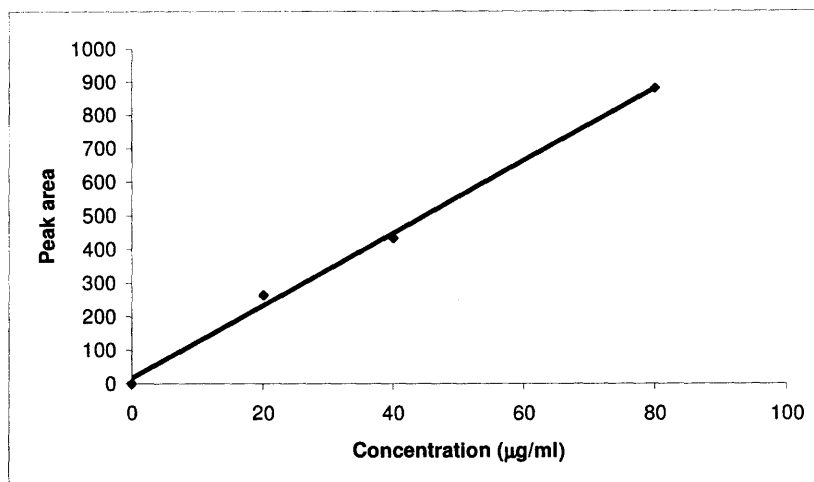


**Figure 2.7** Calibration curve for nicotine.

### 2.10 Calculations for Membrane Permeability, Agent Flux and its Accumulation

The permeation parameters of the agent were calculated by plotting the cumulative corrected amounts ( $\mu\text{g}/\text{cm}^2$ ) of the drug permeated through the membrane versus time (hr). Calculation of the membrane penetration parameters was based on the assumption that the amount of enhancer applied on the membrane is small, hence, there was minimal effect on the solubility of the agent. The slope of the linear portion of the graph provided average flux value ( $J$ ) at steady state ( $\mu\text{g}/\text{cm}^2\text{-hr}$ ).

Permeability ( $P$ , cm/hr) was calculated by:

$$\frac{\Delta C_{receptor}}{\Delta t \times A_{receptor}} \times \frac{V_{receptor}}{C_{donor}} \quad (2.2)$$

$\Delta C_{receptor}$  ( $\mu\text{g}/\text{ml}$ ): the difference of agent concentration in the receptor part in the given time  $\Delta t$  (hr);  $C_{donor}$  ( $\mu\text{g}/\text{ml}$ ): agent concentration in the donor part;  $A$ : diffusional area

(cm<sup>2</sup>). For agent suspension for donor solution, it is the total concentration of both soluble and insoluble agent.

Statistical analysis was performed using one-way analysis of variance (one way ANOVA).

## CHAPTER 3

### RESULTS AND DISCUSSION

#### 3.1 Experimental Results of *In Vitro* Delivery of Doxycycline HCl Based on a Porous Membrane-Based Aqueous-Organic Partitioning System

##### 3.1.1 Distribution Coefficient

The effective distribution coefficient  $K$  for doxycycline HCl between 1-octanol and water was found to be 30, while that between light mineral oil and water was 0.13. Here  $K$  is defined as

$$K = \frac{\text{Concentration of agent in organic phase}}{\text{Total concentration of agent in aqueous phase}} \quad (3.1)$$

In water doxycycline HCl exists as the undissociated compound (Doxy), the dissociated doxycycline  $H^+$  (Doxy $H^+$ ) plus dimers. The sum of these concentrations is the total agent concentration used in the definition of  $K$  Equation (3.1). The agent concentration in organic phase includes dissolved plus suspended amounts.

##### 3.1.2 Release Profiles from Polymeric Membranes Using 1-Octanol and Light Mineral Oil as Vehicles

Two different kinds of polymeric membranes were studied: hydrophobic Celgard<sup>®</sup> 2400 and hydrophilic PVDF. All experiments used either 1-octanol or light mineral oil as the solvent for the agent in either two reservoirs-based cell or Franz diffusion cell.

**3.1.2.1 Release from Celgard<sup>®</sup> 2400 Membrane in Two Reservoirs-Based Cell.** For the release from a 1-octanol-based reservoir system with Celgard<sup>®</sup> 2400 membrane, in the beginning, the change of concentration in the receiving reservoir was proportional to



time (Figure 3.1). Thus it was a zero order release for this period (Guy et al., 1989; Farrell et al., 1997); a straight line behavior was observed. Then a first order release was observed with the characteristics of a quadratic curve (Figure 3.2) (Guy et al., 1989; Farrell et al., 1997). It should be noted that zero order release can be continued for longer lengths of time if the agent concentration in the receiver solution were much smaller (as would be true in *in vivo* studies).

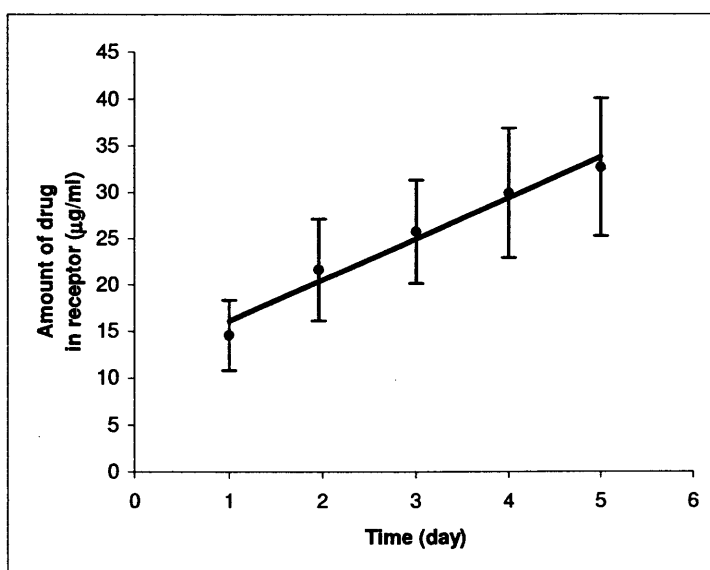


**Figure 3.1** Controlled release of doxycycline HCl through Celgard<sup>®</sup> 2400 membrane in the two reservoirs-based controlled release cell for the first five days (reservoir solvent, 1-octanol. Sol.2).

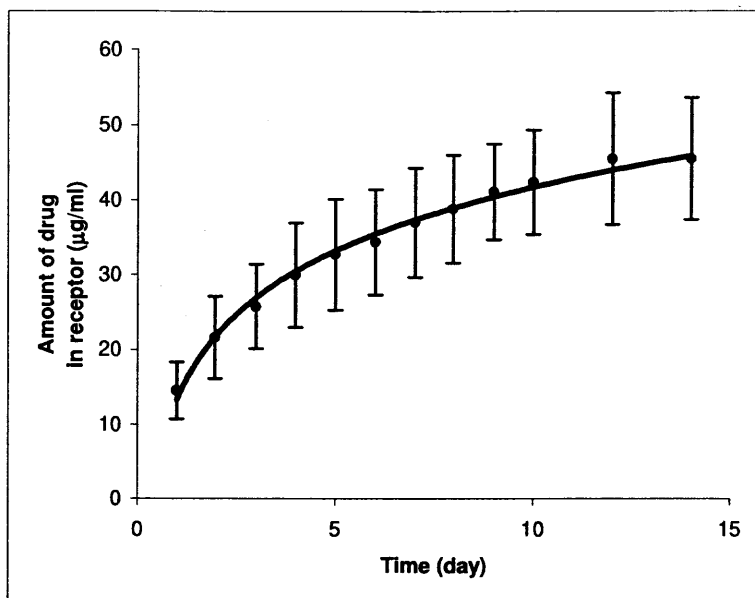


**Figure 3.2** Controlled release of doxycycline HCl through Celgard<sup>®</sup> 2400 membrane in the two reservoirs-based controlled release cell for fourteen days (reservoir solvent, 1-octanol. Sol.2).

**3.1.2.2 Release from PVDF Membrane.** The hydrophilic PVDF membrane was tried next to compare its release characteristics with those of Celgard<sup>®</sup> 2400. For this membrane, Franz diffusion cells were used. The results of release are presented in Figure 3.3. Table 3.1 illustrates the permeation data from different systems.

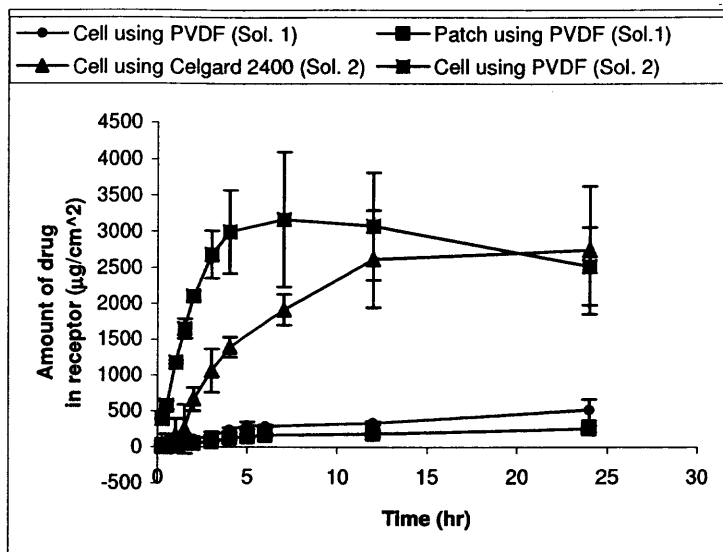


**Figure 3.3** *In vitro* release of doxycycline HCl using 1-octanol as vehicle through PVDF or Celgard® 2400 membrane over 24 hr.

**Table 3.1** Permeation Data Using 1-Octanol as Vehicle for Different Diffusion Systems

Diffusion systems	Permeability (cm/hr)	Flux ( $\mu\text{g}/\text{cm}^2\text{-hr}$ )	$Q_{24}^a$ ( $\mu\text{g}/\text{cm}^2$ )
Two reservoirs-based cell system using Celgard® 2400 membrane (Sol.2)	$0.002 \pm 0.0003$	$18 \pm 3$	$1150 \pm 300$
Franz diffusion cell using Celgard® 2400 membrane (Sol. 2)	$0.014 \pm 0.0006$	$139 \pm 6$	$2750 \pm 890$
Franz diffusion cell using PVDF membrane (Sol. 1)	$0.015 \pm 0.003$	$73 \pm 12$	$516 \pm 150$
Franz diffusion cell using PVDF membrane (Sol. 2)	$0.015 \pm 0.002$	$150 \pm 22$	$2520 \pm 540$
Hill Top® patch using PVDF membrane (Sol.1)	$0.007 \pm 7.14\text{E-}05$	$36.0 \pm 0.4$	$395 \pm 3$

<sup>a</sup> $Q_{24}$ , receptor concentration after 24 hr.

Obviously, the PVDF membrane has a somewhat higher permeability and flux than Celgard® 2400. Theoretically, based on Fick's First Law, the formula of flux of the permeating species can be expressed as (Kessler et al., 1992, 2001):

$$J = D_{eff} \frac{\Delta C}{l} = \frac{D_{eff}}{l} (C_{1D} - C_{1R}) = \frac{D_{eff}}{l} \left( \frac{C_{1D}^{oct}}{K} - C_{1R} \right) \quad (3.2)$$

in which,  $K$  is the partition coefficient,  $D_{eff}$  is the effective diffusion coefficient in the membrane,  $\Delta C$  is the concentration difference in the pore liquid of the two external solution-pore liquid interfaces on two sides:  $C_{1D}$  is the concentration in the pore liquid on the donor side and  $C_{1R}$  is that on the receptor side;  $l$  is the membrane thickness. The last formula is utilized in the following calculation with  $C_{1R} \cong 0$ , effectively zero concentration in the reservoir vessel having an aqueous phase; the donor chamber has the organic phase.

The partition coefficient  $K$  of the agent between the reservoir organic solvent 1-octanol and water is the same in the case of membranes, Celgard® 2400 and PVDF. The effective diffusion coefficient of the drug through water in the porous membrane may be defined as (Prasad et al., 1988):

$$D_{eff} = \frac{D_{water} \epsilon_m}{\tau_m} \quad (3.3)$$

in which  $\epsilon_m$  and  $\tau_m$  are the porosity and tortuosity of the membrane, respectively, and  $D_{water}$  is the diffusion coefficient in free solution. For Celgard®,  $\epsilon_m=0.38$  and  $\tau_m=5$  whereas for PVDF,  $\epsilon_m=0.7$  and  $\tau_m=2.58$ . Therefore  $(D_{eff}/l)$  factor in Equation (3.2) is essentially the same for both Celgard® 2400 and PVDF films  $((\epsilon_m/\tau_m)l): \frac{0.38}{5 \times 25}$

( $=0.0030\mu\text{m}^{-1}$ ) for the Celgard<sup>®</sup> 2400 film and  $\frac{0.7}{2.58 \times 100}$  ( $=0.0027\mu\text{m}^{-1}$ ) for the PVDF film).

There are two species of doxycycline drug in the aqueous phase, the undissociated doxycycline (Doxy) and doxycycline  $\text{H}^+$  (Doxy $\text{H}^+$ ). There are two unknowns here whose values are needed before the total agent flux can be calculated. First, the relative distribution between the two species has to be determined. Second, their diffusion coefficients also need to be known. The first dissociation equilibrium constant  $K_1$  for doxycycline  $\text{H}^+$  is  $10^{-3.3}$  (Libinson, 1977):

$$K_1 = 10^{-3.3} = \frac{[\text{Doxy}] \cdot [\text{H}^+]}{[\text{DoxyH}^+]} \quad (3.4)$$

The transport analysis is based on the following assumptions: (1) The agent DoxyHCl is completely dissociated in water into Doxy $\text{H}^+$  and  $\text{Cl}^-$ . (2) Doxy $\text{H}^+$  is the protonated form of the original base Doxy. (3) Dimerization of both Doxy $\text{H}^+$  and Doxy are neglected due to the low value of the total agent concentration  $C_T \sim 6.9 \times 10^{-4}$  M (Bogardus et al., 1979).

Since the pores contained only an aqueous solution of Doxy $\text{H}^+$ ,  $[\text{Doxy}] \equiv [\text{H}^+]$ . For a total agent concentration of Sol. 2 of  $10^4 \mu\text{g/ml}$ ,  $C_T$  is

$$C_T = C_{\text{Doxy}} + C_{\text{DoxyH}^+} = \frac{C_{\text{Doxy}}}{K} = \frac{10^4}{30} \mu\text{g/ml} = 6.94 \times 10^{-4} \text{ mol/l} \quad (3.5)$$

The following values were obtained by the solution of a quadratic equation obtained from Equations (3.4) and (3.5):  $C_{\text{Doxy}}=157 \mu\text{g/ml}$  and  $C_{\text{DoxyH}^+}=176 \mu\text{g/ml}$ . It was assumed that their concentration in the receptor was zero. Hence, the total agent flux was:

$$J = \frac{D_{\text{Doxy}} \cdot \epsilon_m}{l \cdot \tau_m} (C_{\text{Doxy}} - 0) + \frac{D_{\text{DoxyH}^+} \cdot \epsilon_m}{l \cdot \tau_m} (C_{\text{DoxyH}^+} - 0) \quad (3.6)$$

The diffusion coefficients of doxycycline in free solution ( $D_{\text{Doxy,water}}$ ) can be obtained from the Wilke-Chang Equation (Wilke et al., 1955) and is equal to  $3.93 \times 10^{-6}$   $\text{cm}^2/\text{sec}$ . The diffusion coefficient of  $D_{\text{DoxyH}^+}$  is to be obtained from considerations of diffusion potential-based diffusion coefficient  $D_{\text{DoxyH}^+\text{Cl}^-}$  obtained from the individual values of  $D_{\text{DoxyH}^+}$  and  $D_{\text{Cl}^-}$  and their charges (Newman, 1973):

$$D_{\text{DoxyH}^+\text{Cl}^-} = \frac{D_{\text{DoxyH}^+} \cdot D_{\text{Cl}^-} (z_+ - z_-)}{(z_+ \cdot D_{\text{DoxyH}^+} - z_- \cdot D_{\text{Cl}^-})} \quad (3.7)$$

$D_{\text{DoxyH}^+}$  for this calculation is assumed essentially equal to  $3.93 \times 10^{-6}$   $\text{cm}^2/\text{sec}$  corresponding to the undissociated  $D_{\text{Doxy}}$ . Here  $z_+ = +1$ ,  $z_- = -1$  and  $D_{\text{Cl}^-} = 2.03 \times 10^{-5}$   $\text{cm}^2/\text{sec}$  (Newman, 1973), so that

$$D_{\text{DoxyH}^+\text{Cl}^-} = \frac{3.93 \times 10^{-6} \times 2.03 \times 10^{-5} [1 - (-1)]}{3.93 \times 10^{-6} - (-2.03 \times 10^{-5})} = 6.59 \times 10^{-6} \text{ cm}^2/\text{sec}$$

Therefore for the Celgard<sup>®</sup> 2400 film, the total flux of doxycycline HCl in both forms from Equation (3.6) is:

$$J = [(3.93 \times 10^{-6}) \cdot (0.003 \times 10^4) \cdot (157 - 0) + (6.59 \times 10^{-6}) \cdot (0.003 \times 10^4) \cdot (176 - 0)] \times 3600 \\ \cong 191.9 \mu\text{g} / \text{cm}^2 \cdot \text{hr}$$

Since the concentrations in the receptor part were always much less than the donor part and the receptor side was well mixed,  $C_{IR}$  was assumed to be 0 for all species for flux calculation by Equation (3.6). (The value of J without consideration of ionization

is  $135.9 \mu\text{g}/\text{cm}^2\text{-hr}$ .) Results of the theoretical flux values (J) obtained when values of all the experimental parameters were introduced into Equation (3.6), are shown in Table 3.2. This table also includes the corresponding experimentally observed values.

**Table 3.2** Comparison of Calculated Flux Values and Experimental Ones

Membrane	Solution	Calculated value $\mu\text{g}/\text{cm}^2\text{-hr}$	Experimental value $\mu\text{g}/\text{cm}^2\text{-hr}$
Celgard <sup>®</sup> 2400 membrane	Sol. 2 (2 reservoir-based cell)	21.3	18±3
	Sol. 2 (Franz cell)	191.9	139±6
PVDF membrane	Sol. 1 (Franz cell)	86.4	73±12
	Sol. 2 (Franz cell)	172.7	150±22

Obviously, the flux results from the experimental data are quite close to those calculated from the model equation. For the flux from the 2 reservoir-based cell, however, with no stirring in the receptor part, the existing stagnant layer in such a system has to be considered. As shown in Figure 2.1, two small donor cells immersed in a 200 ml reservoir may be considered in analogy to the diffusion from a droplet to a stagnant fluid around it. From the volume of each cell ( $0.9 \text{ cm}^3$ ), the characteristic dimension of an equivalent sphere is 1.2 cm. The Sherwood number (Sh) for this case is 2 (Welty et al., 1976). Therefore, the mass transfer coefficients,  $k_{\text{Doxy}}$  and  $k_{\text{DoxyH}^+}$ , are:

$$\begin{cases} k_{\text{Doxy}} = \frac{D_{\text{Doxy}} \times Sh}{d} = \frac{3.93 \times 10^{-6} \times 2}{1.2} = 6.55 \times 10^{-6} \text{ cm/s} \\ k_{\text{DoxyH}^+} = \frac{D_{\text{DoxyH}^+} \times Sh}{d} = \frac{6.59 \times 10^{-6} \times 2}{1.2} = 10.98 \times 10^{-6} \text{ cm/s} \end{cases} \quad (3.8)$$

Introducing these values into the flux Equation (3.6), one obtains:

$$\begin{aligned}
 J &= (k_{Doxy} \times \Delta C_{Doxy} + k_{DoxyH^+} \times \Delta C_{DoxyH^+}) \times 3600 \text{ sec/hr} \times 2 \\
 &\cong 21.3 \mu\text{g/cm}^2 \cdot \text{hr}
 \end{aligned}
 \tag{3.9}$$

which is close to the experimental value. It is to be noted that the permeabilities calculated by Equation (2.2) utilized the total solute concentration in the organic solvent in the reservoir. If the corresponding aqueous phase solubility is used as the value of  $C_{\text{donor}}$ , it will be much lower for 1-octanol; therefore the value of permeability P will go up. For light mineral oil considered later, it will go down since K for light mineral oil is 0.13. Note furthermore, that for the dispersion in light mineral oil,  $C_{\text{donor}}$  included both soluble and insoluble doxycycline HCl.

The results of transport for the patch system identified at the end of Table 3.1 will be considered now. It is clear that all of the permeation parameters of the patch system are lower than those from the Franz diffusion cell for the same PVDF membrane. It may be justified by the fact that the patch system was more complex with a number of uncertainties compared to the Franz cell with the membrane mounted. In the case of the patch, the membrane was sealed to the agent reservoir by an adhesive; the extent of agent absorption in the adhesive was unknown. Given other uncertainties such as bubbles created during patch preparation (difficult to remove during experiments) and unexpected leaks from the periphery of reservoir, it is not surprising that the release rate from the first sample of patch was not as good as those from the Franz diffusion cell system.

To improve the permeability, the patch system was optimized: instead of filling the agent suspension directly in the reservoir, it was transferred into a double layer of cotton pad (originally housed in the reservoir of the patch obtained from the manufacturer), then covered with a PVDF membrane. With the cotton pad holding the



agent solution, the chances of peripheral leakage were considerably reduced, the creation of bubbles was avoided, and the patch became a stable release source. For this revised configuration, permeation results were close to those of its relevant membrane system as shown in Table 3.3 and Figure 3.4.

**Table 3.3** Permeation Data Using Light Mineral Oil as Vehicle from Different Diffusion Systems

Diffusion systems	Permeability (cm/hr)	Flux ( $\mu\text{g}/\text{cm}^2\text{-hr}$ )	$Q_{24}$ ( $\mu\text{g}/\text{cm}^2$ )
Franz diffusion cell using PVDF membrane	$0.03 \pm 0.006$	$146 \pm 27$	$1440 \pm 240$
Hill Top <sup>®</sup> patch using PVDF membrane	$0.004 \pm 0.0008$	$22 \pm 4$	$267 \pm 22$
Hill Top <sup>®</sup> patch using PVDF membrane and cotton pad	$0.025 \pm 0.003$	$133 \pm 16$	$885 \pm 250$

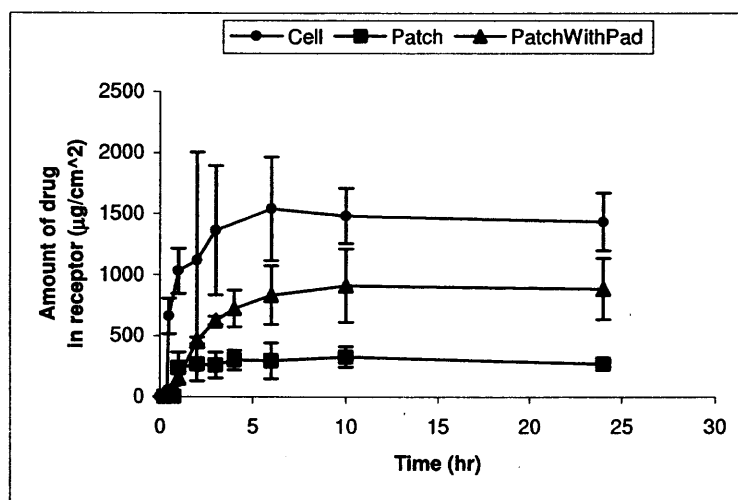


**Figure 3.4** *In vitro* release of doxycycline HCl using light mineral oil as vehicle through PVDF membrane over 24 hr.

Since hydrophobic Celgard<sup>®</sup> 2400 films needed several days of pretreatment to get wetted for use, hydrophilic PVDF membrane was used in the following experiments. The solvent, 1-octanol, has a strong odor; therefore, light mineral oil was employed to test whether it would be a good replacement with light color and odorless property. Figure 3.4 shows the controlled release profiles from the Franz cell system and the patch-based system; Table 3.3 gives the permeation data results from these setups.

On comparing these results with those based on 1-octanol (Table 3.1), it is observed that the permeation parameter is halved using 1-octanol; further the fluxes are close to each other although much less solute was dissolved in the light mineral oil (around 550  $\mu\text{g/ml}$ ) compared to that in 1-octanol. Applying light mineral oil as the vehicle actually decreases the solubility of the agent strongly compared to 1-octanol; it forms a suspension, which decreases the agent concentration in the solvent for partitioning into water in the membrane pores. However, the distribution coefficients for the agent between 1-octanol/water and mineral oil/water are 30 and 0.13, respectively. It is the principal reason why in light mineral oil system, this antibiotic has a much higher permeability. Therefore, the solvent choice was narrowed down to light mineral oil for the experiments to be described next.

With these results, it is clear that a porous polymeric membrane in an aqueous-organic partitioning system should not be a major obstacle for the agent to pass through. Therefore, in the next part, a mouse skin was used for test with the polymeric membrane on top of it.

### 3.2 Experimental Results of *In Vitro* Drug Delivery Based on a Porous Membrane-Based Aqueous-Organic Partitioning System through Mouse Skin

#### 3.2.1 Release Profiles of Doxycycline HCl from Porous Polymeric Membrane and Mouse Skin Using 10% Ethanol in Light Mineral Oil as Vehicle in the Reservoir

First, two control experiments were made: controlled release through the mouse skin without any polymeric membrane and through both polymeric membrane and mouse skin. Since the agent is a polar drug having a relatively higher molecular weight, 10% ethanol was used to enhance its transporting ability through skin. These release profiles are shown in Figure 3.5, and the permeation parameters are given in Table 3.4.

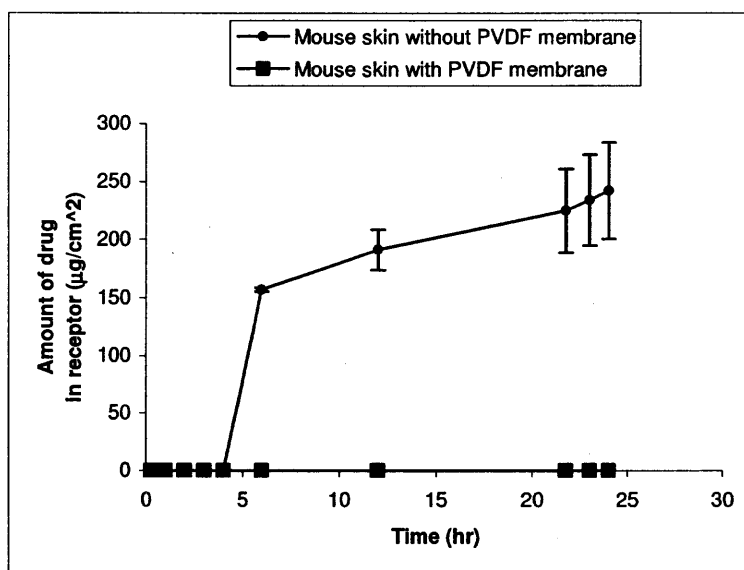


**Figure 3.5** *In vitro* release of doxycycline HCl through mouse skin with and without PVDF membrane over 24 hr.

**Table 3.4** Permeation Data\* through Mouse Skin with and without PVDF Membrane

Diffusion systems	Permeability (cm/hr)	Flux ( $\mu\text{g}/\text{cm}^2\text{-hr}$ )	$Q_{24}$ ( $\mu\text{g}/\text{cm}^2$ )
Hairless mouse skin only without PVDF membrane	0.001 $\pm$ 0.0002	9.8 $\pm$ 2.1	240 $\pm$ 40
Hairless mouse skin with PVDF membrane	0	0	0

\* Mineral oil in donor reservoir has 10% ethanol.

It is clear that a significant drug permeation rate was achieved through the skin; however, apparently there was essentially no agent going through the skin after passing through the aqueous pores of the PVDF membrane. The reason is likely to be as follows. In the case of the bare skin, the light mineral oil based solution was directly in contact with the skin. The light mineral oil-based swelling of the skin facilitated the drug transport. However, when the water-filled pores of the PVDF membrane was imposed in between, there was no such facilitation since the skin was no longer exposed to light mineral oil. The stratum corneum of the skin is expected to be a difficult medium for such a polar agent to go through unless facilitated by some means.

Next, three kinds of enhancers were investigated: azone (amide), cineole (terpene) (Godwin et al., 1999; El-Kattan et al., 2000; El-Kattan et al., 2001), and linoleic acid (fatty acid) in different percentage concentrations: 5%, 10%, 20% v/v. For the groups including azone and cineole acid, respectively, very little of the agent accumulated in the receptor, while the agent permeability and flux were close to zero. Only linoleic acid as an enhancer yielded reasonable results as shown in Figure 3.6 and Table 3.5. A patch system filled with 10% linoleic acid as enhancer was tried and yielded similar results in the Franz diffusion cell system; these results are also included in this figure and table. In

order to make the patch perform as well as the diffusion cell, the PVDF membrane was mounted on the patch with epoxy two days before the diffusion experiment through the mouse skin. In Table 3.5, data from a research group using human cadaver skin (Perkins et al., 1999) are also listed for the purpose of comparison.

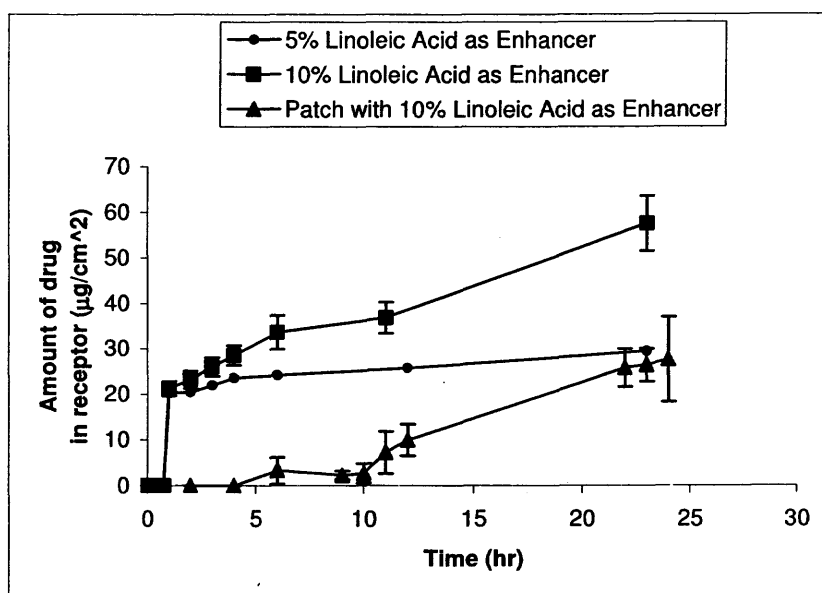


**Figure 3.6** *In vitro* release profile of doxycycline HCl with linoleic acid as enhancer through PVDF membrane and mouse skin over 24 hr.

**Table 3.5** Permeation Data through PVDF Membrane and Mouse Skin with Different Amounts of Linoleic Acid and through a Human Cadaver Skin\*

Diffusion systems	Permeability (cm/hr)	Flux ( $\mu\text{g}/\text{cm}^2\text{-hr}$ )	$Q_{24}$ ( $\mu\text{g}/\text{cm}^2$ )
5% linoleic acid in drug solution	$1.6\text{E-}04 \pm 3.2\text{E-}05$	$1.6 \pm 0.3$	$37 \pm 2$
10% linoleic acid in drug solution	$2.7\text{E-}04 \pm 5.0\text{E-}05$	$2.7 \pm 0.5$	$63 \pm 9$
10% linoleic acid in drug patch	$1.7\text{E-}04 \pm 1.5\text{E-}05$	$1.7 \pm 0.2$	$28 \pm 10$
Doxycycline HCl across full-thickness human cadaver skin from ethanol vehicle*	$4.8\text{E-}06 \pm 5\text{E-}07$	$0.13 \pm 0.01$	$20^*$

\* Perkins et al. (1999) have not given this data directly, and the number here was calculated from their Figure 2 on the amount permeated versus time.

Due to its long-chain double bond structure similar to lipid bilayer of skin, linoleic acid is believed to disrupt the skin lipid packing and make them (lipids) more dynamic (Chattaraj et al., 1995). This could explain why linoleic acid has significant effect on the agent permeation in the current investigation.

Mouse skin was used in this experiment since this was an initial feasibility study. It is known, however, that data from mouse skin provide higher permeability values than would be observed in human cadaver skin (Roy et al., 1994; Ghosh et al., 2000; Sagar et al., 2001). Mouse skin in general is much thinner than human cadaver skin and also possesses a different lipid composition within the stratum corneum. In view of the data from a previously published cadaver skin experiment (Perkins et al., 1999), it is expected that application of the membrane-skin system with aqueous-organic partitioning to a human skin *in vitro* would result in a reasonable flux.

In addition to the 24-hour release, 120-hour long term release experiments have also been carried out. The permeation data were similar to those from the 24-hour results with steady releasing rate achieved. These results suggest that it is possible to transfer this system to a transdermal patch later. Figure 3.7 shows the extended-time release profile.

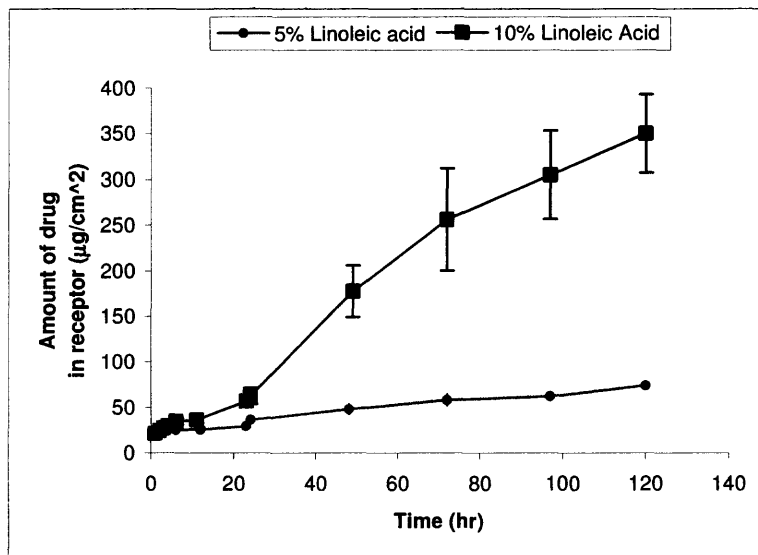


**Figure 3.7** *In vitro* release profile of doxycycline HCl with linoleic acid as enhancer through PVDF membrane and mouse skin over 120 hr.

### 3.2.2 Release Profiles of Caffeine and Nicotine from Porous Polymeric Membrane and Mouse Skin Using 1-Octanol and Light Mineral Oil as Vehicle Respectively in the Reservoir

To further test whether such a system works for other agents, two small polar drugs, caffeine and nicotine of relatively smaller MWs (194.2 and 162), were also used. The release profiles are shown in Figure 3.8 and Figure 3.9, respectively; their permeation data are provided in Table 3.6. It is not surprising that, without any enhancer to facilitate their transport, the permeation data for both agents were more than three times than those from a similar system for doxycycline HCl.

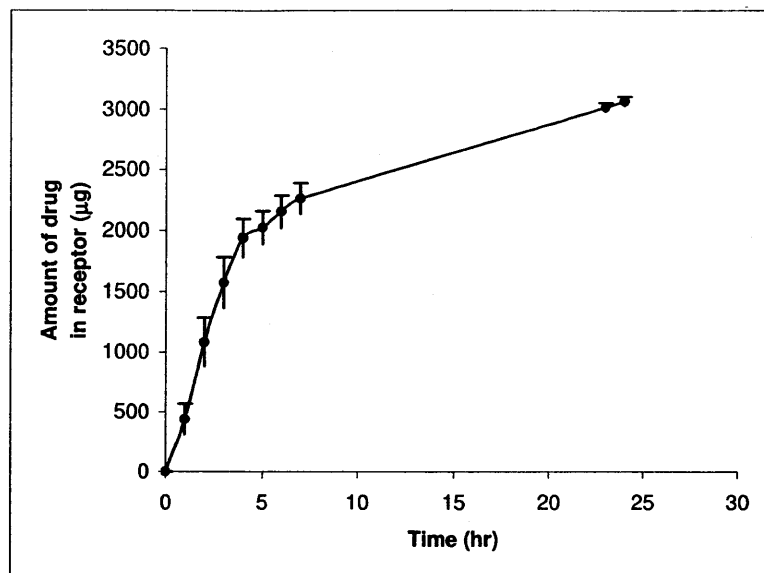


**Figure 3.8** *In vitro* release profile of caffeine with 1-octanol as vehicle through PVDF membrane and mouse skin over 24 hr.

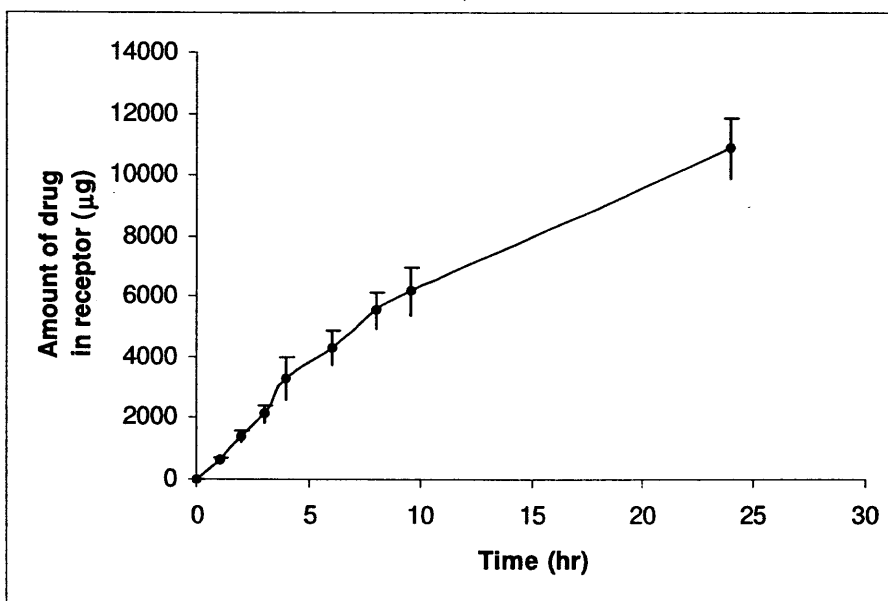


**Figure 3.9** *In vitro* release profile of nicotine with light mineral oil as vehicle through PVDF membrane and mouse skin over 24 hr.



**Table 3.6** Permeation Data of Small Polar Agents through PVDF Membrane and Mouse Skin without Any Enhancer

Diffusion systems	Permeability (cm/hr)	Flux ( $\mu\text{g}/\text{cm}^2\text{-hr}$ )	$Q_{24}$ ( $\mu\text{g}/\text{cm}^2$ )
Caffeine suspension in 1-octanol	0.09 $\pm$ 0.01	892 $\pm$ 62	4820 $\pm$ 48
Nicotine solution in light mineral oil	0.12 $\pm$ 0.02	1180 $\pm$ 189	17100 $\pm$ 1520

### 3.3 Experimental Results of *In Vitro* Drug Delivery through Mouse Skin Using Conductive Membrane as an Electrode

The results of characterization of PANi films needed for characterizing the membrane transport of various agents through the PANi films are presented first. The permeation study is focused initially on agents in their aqueous solution because it is a new application of PANi in the area of iontophoretic TDD. Without this knowledge, the behavior in aqueous-organic partitioning system cannot be explained. The release profiles through PANi membrane of three solutes, e.g., caffeine, lidocaine HCl and doxycycline HCl from their aqueous solutions are then illustrated. Next, the release rates are determined from Fick's law of diffusion and compared with the data. The data obtained when a mouse skin is added to the PANi film are analyzed subsequently. This has been followed by iontophoretic study of the composite of PANi film and a mouse skin using two different kinds of electrodes: one based on a conventional Ag|AgCl electrodes and the other being based on PANi|AgCl. Finally, doxycycline HCl release based on an aqueous-organic partitioning system is explored.

### 3.3.1 Properties of PANi Membranes

The thickness of the PANi films was found to be  $0.018 \text{ mm} \pm 0.002 \text{ mm}$ . The porosity of PANi films was found to be  $0.67\% \pm 0.08\%$  based on the measurements of three films. The membrane porosity ( $\epsilon_m$ ) is quite low with potential contributions from some defects; introduction of low levels of pore forming agents in the casting solution would have led to higher porosity.

The value of the PANi membrane parameter ( $\epsilon_m/\tau_m$ ), where  $\tau_m$  is the membrane tortuosity, was found to be  $9\text{E-}4 \pm 7\text{E-}5$  from an average of nine films by measuring fluxes under different donor concentrations of caffeine solutions.

Combining Equations (3.2) and (3.3), the equation of flux (J) is changed to:

$$J = \frac{D_{\text{water}} \cdot \epsilon_m}{\tau_m \cdot l} (C_{1D} - C_{1R}) \quad (3.10)$$

Therefore, the value of the membrane parameter ( $\epsilon_m/\tau_m$ ) can be expressed as:

$$\frac{\epsilon_m}{\tau_m} = J \cdot \frac{l}{D_{\text{water}}} \cdot \frac{1}{(C_{1D} - C_{1R})} \quad (3.11)$$

Next, three caffeine solutions of different concentrations were prepared: 5, 10, 20.4 mg/ml. From each solution in donor part, a flux value was obtained and used in Equation (3.11) to calculate the membrane's ( $\epsilon_m/\tau_m$ ); the averaged value,  $9\text{E-}4$ , was used in later calculations.

In addition to the thickness (l) as a known value, the diffusion coefficient of caffeine in free solution ( $D_{\text{Caf,water}}$ ) was obtained from the Wilke-Chang Equation (Wilke et al., 1955):

$$D_{Caf,water} = 7.4 \times 10^{-8} \frac{(\phi M_{Water})^{0.5} T}{\eta_{Water} V_{Caffeine}^{0.6}} \quad (3.12)$$

where  $M_{Water}$ ,  $\eta_{Water}$ ,  $V_{Caffeine}$ ,  $\phi$  and  $T$  are the molecular weight, viscosity of water, molar volume of caffeine, association factor of water (2.6) and temperature, respectively. The molar volume is equal to 159.3, and the value of  $D_{Caf,water}$  is  $7.08 \times 10^{-6} \text{ cm}^2/\text{s}$ .

Table 3.7 lists this film's ( $\epsilon_m/\tau_m$ ) calculated from different flux levels for different donor concentrations; the averaged value was used in the following calculations.

**Table 3.7** The Value of PANi Membrane Parameter ( $\epsilon_m/\tau_m$ ) Calculated from Data of Different Fluxes for Caffeine\*

Concentration of caffeine (mg/ml)	Flux ( $\mu\text{g}/\text{cm}^2 \text{ h}$ )	$\epsilon_m/\tau_m$	Avg. ( $\epsilon_m/\tau_m$ )
5	66.6	0.00094	9E-4±7E-5
10	136.2	0.00096	
20.4	239.5	0.00083	

\* Using Equation (3.11).

### 3.3.2 Aqueous Solution System

**3.3.2.1 Release Profiles from PANi Membranes.** The results of the release of three agents through PANi membrane as obtained in the Franz cell are presented in Table 3.8; the results illustrate the permeation data for three different agents in terms of their permeability, flux and 24-hr accumulation values. Obviously, doxycycline HCl, as the agent having the largest MW among the three, had the least flux, permeability and accumulation. Between caffeine and lidocaine HCl, although caffeine has a small MW, it is believed that the higher concentration of lidocaine HCl in the donor solution (by a factor of two) played a critical role in providing almost a doubled flux and six times accumulation compared to those for caffeine. The following calculations provide a justification for these results.

**Table 3.8** Permeation Data for Three Agents Released through PANi Membrane

Agent	Permeability (cm/hr)	Flux ( $\mu\text{g}/\text{cm}^2 \text{ hr}$ )	$Q_{24}$ ( $\mu\text{g}/\text{cm}^2$ )
Caffeine	1.2E-2 $\pm$ 9.0E-3	240 $\pm$ 177	570 $\pm$ 250
Lidocaine HCl	1.1E-2 $\pm$ 3.5E-3	461 $\pm$ 147	3330 $\pm$ 1760
Doxycycline HCl	3.5E-3 $\pm$ 7.0E-4	72 $\pm$ 14	307 $\pm$ 100

Conventionally, the value of the flux of the permeating species may be obtained by simple diffusion through the membrane pores (Kessler et al., 1992, 2001):

$$J = D_{eff} \frac{\Delta C}{l} = \frac{D_{eff}}{l} (C_{1D} - C_{1R}) \quad (3.13)$$

in which,  $D_{eff}$  is the effective diffusion coefficient in the membrane,  $\Delta C$  is the concentration difference in the pore liquid of the two external solution-pore liquid interfaces on two sides:  $C_{1D}$  is the concentration in the pore liquid of the donor side and  $C_{1R}$  is that in the receptor side;  $l$  is the membrane thickness. The last formula is utilized in the following calculation with  $C_{1R} \cong 0$ , effectively zero concentration in the receiver vessel having an aqueous phase; for the donor chamber,  $C_{1D} \cong C$ , which is the agent concentration in the donor solution. The partition coefficient  $K$  of the agent between the reservoir liquid (aqueous solution) and pore liquid (aqueous solution) is assumed to be 1.

The effective diffusion coefficient of the agent through water in the porous membrane may be defined as (Prasad et al., 1988)

$$D_{eff} = \frac{D_{H_2O} \varepsilon}{\tau_m} \quad (3.14)$$

Wilke-Chang (Wilke et al., 1955) estimation method for diffusion coefficient in free solution was used to calculate  $D_{water}$  of different agents. Since the concentrations in the receptor part were always much less than those in the donor part and the receptor side was well mixed,  $C_{IR}$  was assumed to be 0 for the following calculations. The implications of ionization on the partitioning behavior considered earlier in Equations (3.4) to (3.6) were also considered in such calculations. As for doxycycline HCl, since the donor solution concentration was higher than 0.01 M, its dimerized form was included in the calculation of its model flux value as well (Bogardus et al., 1979). Therefore, the value of the flux in the model calculations has contributions from three components: flux of the base ( $J_{Doxy}$ ), flux of the protonated base ( $J_{DoxyH^+}$ ) and flux of its dimer ( $J_{dimer}$ ). As for lidocaine HCl, however, such data for its dimerization are not available in literature, therefore a general calculation was carried out in the manner shown in Equations (3.4) to (3.6). Results of model flux predictions ( $J$ ) obtained when all the experimental parameters were introduced into Equation (3.13), are shown in Table 3.9. This table also includes the corresponding experimentally observed values. Detailed calculations are provided after Table 3.9.

**Table 3.9** Comparison of Model Predictions and Experimental Flux Data for Three Agents, Caffeine, Lidocaine HCl and Doxycycline HCl

Agent	$D_{water-agent}$ ( $cm^2/s$ )	Model prediction ( $\mu g/cm^2$ hr)	Experimental flux ( $\mu g/cm^2$ hr)
Caffeine	7.08E-6	260	240±180
Lidocaine HCl	7.91E-6	573	461±150
Doxycycline HCl	6.59E-6	198	72±14

## (1) Model flux of caffeine

Since caffeine is a neutral molecule which does not produce any charged ions in solution, its flux is determined simply by using its concentration values in Equation (3.13), where the donor solution concentration of caffeine is 20400  $\mu\text{g/ml}$ ,

$$\begin{aligned}
 J &= \frac{D_{\text{eff}}}{l} (C_{1D} - C_{1R}) \\
 &= \frac{7.08 \times 10^{-6}}{0.0018} \times 0.0009 \times (20400 - 0) \times 3600 \\
 &\cong 260.0 \mu\text{g} / \text{cm}^2 \text{h}
 \end{aligned} \tag{3.15}$$

## (2) Model flux of doxycycline HCl

How to calculate the model flux value of an ionizable salt agent has been described earlier via Equations (3.4) to (3.6). Since the concentration of doxycycline HCl was quite high (0.0425 M), the role of its dimerization has to be considered also in the flux calculation (Bogardus et al., 1979), which was neglected earlier (Equation (3.6)).

There are four species of doxycycline agent in the aqueous phase; the formula symbol of each and its concentration are indicated in separate brackets: the original base doxycycline (Doxy) ( $C_{\text{Doxy}}$ ), doxycycline  $\text{H}^+$  (Doxy $\text{H}^+$ ) ( $C_{\text{DoxyH}^+}$ ), doxycycline dimers (Doxy $\text{H}^+$ )<sub>2</sub> ( $C_{\text{di}}$ ) or (Doxy)<sub>2</sub> $\text{H}^+$  ( $C_{\text{di}}$ ) (Bogardus et al., 1979).

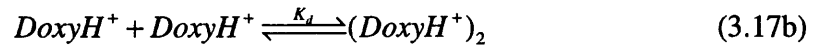
First, the total concentration  $C_T$  of doxycycline in all forms was related to the total concentration ( $C_m$ ) of Doxy ( $C_{\text{Doxy}}$ ) and Doxy $\text{H}^+$  ( $C_{\text{DoxyH}^+}$ ) as the monomer form of doxycycline by the equation from Bogardus et al. (Bogardus et al., 1979):

$$C_T = C_m + 2K_d C_m^2 \tag{3.16}$$

where  $K_d$  is the dimerization constant and equal to 24 (Bogardus et al., 1979); here

$$C_T = C_m + C_{di} = 20400 \mu\text{g} / \text{ml} = 0.0425 \text{mol} / \text{l} \quad (3.17a)$$

where  $C_{di}$  is the concentration of doxycycline dimers. Note that the dimerization equation is (Bogardus et al., 1979):



By solving Equation (3.16) for this value of  $C_T$ ,

$$C_m = C_{\text{Dox}y} + C_{\text{Dox}yH^+} = 0.0211M \quad (3.18)$$

$$C_{di} = 0.0214M = 10274 \mu\text{g} / \text{ml} \quad (3.19)$$

From Equation (3.18), the concentration values of each monomer form of doxycycline were obtained by the solution of a quadratic equation obtained from Equation (3.4) (Libinson, 1977):

$$K_1 = 10^{-3.3} = \frac{[\text{Dox}y] \cdot [H^+]}{[\text{Dox}yH^+]} \quad (3.4)$$

By solving Equation (3.4) together with Equation (3.18),

$$C_{\text{Dox}y} = 3.01 \times 10^{-3} M = 1445 \mu\text{g} / \text{ml}, \text{ and } C_{\text{Dox}yH^+} = 0.0181M = 8685 \mu\text{g} / \text{ml}.$$

Using Wilke-Chang estimation method (Wilke et al., 1955), the diffusion coefficients of monomers and dimers of doxycycline HCl in free solution are (see Section 3.1.2.2 for  $D_{\text{Dox}yH^+, \text{water}}$  and the same method for that of dimers):

$$\begin{cases} D_{Doxy,water} = 3.93 \times 10^{-6} \text{ cm}^2 / \text{s} \\ D_{DoxyH^+,water} = 6.59 \times 10^{-6} \text{ cm}^2 / \text{s} \\ D_{(DoxyH^+)_2,water} = D_{(Doxy)_2H^+,water} = 4.58 \times 10^{-6} \text{ cm}^2 / \text{s} \end{cases} \quad (3.20)$$

The total flux of doxycycline HCl had three components:  $J_{Doxy}$ ,  $J_{DoxyH^+}$  and  $J_{dimer}$ :

$$J = J_{Doxy} + J_{DoxyH^+} + J_{dimer} \quad (3.21)$$

Therefore,

$$J = (3.93 \times 10^{-6} \times 1445 + 6.59 \times 10^{-6} \times 8685 + 4.58 \times 10^{-6} \times 10274) \times 0.50 \times 3600, \quad \text{where} \\ \cong 197.9 \mu\text{g}/\text{cm}^2\text{h}$$

$$\left(\frac{\varepsilon_m}{\tau_m}\right) \cdot \frac{1}{l} = 0.50 \text{ cm}^{-1}.$$

Without consideration of the existence of dimer forms of doxycycline HCl, the predicted value of flux would be  $232.0 \mu\text{g}/\text{cm}^2 \text{ h}$ .

### (3) Model flux of lidocaine HCl

Similarly, the flux of lidocaine HCl should have contributions from three sources. However, the formation of its dimers under the high agent concentration in water of  $0.1485 \text{ M}$  is so far a hypothesis (Beronius, 2004); the following calculation is therefore based on the general method shown in Section 3.1.2.2.

There are two species of lidocaine agent in the aqueous phase, the undissociated lidocaine (Lido) and lidocaine  $\text{H}^+$  (Lido $\text{H}^+$ ). There are two unknowns here whose values are needed before the total agent flux can be calculated. First, the relative distribution between the two species has to be determined. Second, their diffusion coefficients also



need to be known. The first dissociation equilibrium constant  $K_1$  for lidocaine  $H^+$  is  $10^{-7.2}$  (Sjöberg et al., 1996):

$$K_1 = 10^{-7.2} = \frac{[Lido] \cdot [H^+]}{[LidoH^+]} \quad (3.22)$$

For a total agent concentration  $C_T$  of lidocaine HCl,

$$C_T = C_{Lido} + C_{LidoH^+} = 40220 \mu g / ml = 0.1485 mol / l \quad (3.23)$$

The following values were obtained for the individual species by the solution of a quadratic equation obtained from Equation (3.22):  $C_{Lido} = 26 \mu g / ml$  and  $C_{LidoH^+} = 40194 \mu g / ml$ . It was assumed that their individual concentrations in the receptor were zero. Therefore the total agent flux is:

$$J = \frac{D_{Lido}}{l} \cdot \left(\frac{\epsilon_m}{\tau_m}\right) \cdot (C_{Lido} - 0) + \frac{D_{LidoH^+}}{l} \cdot \left(\frac{\epsilon_m}{\tau_m}\right) \cdot (C_{LidoH^+} - 0) \quad (3.24)$$

The diffusion coefficients of lidocaine in free solution ( $D_{Lido, water}$ ) can be obtained from the Wilke-Chang Equation and is equal to  $4.91 \times 10^{-6} \text{ cm}^2 / \text{sec}$ . The diffusion coefficient of  $D_{LidoH^+}$  compound is obtained from considerations of diffusion potential-based diffusion coefficient  $D_{LidoH^+Cl^-}$  obtained from the individual values of  $D_{LidoH^+}$  and  $D_{Cl^-}$  and their charges:

$$D_{LidoH^+Cl^-} = \frac{D_{LidoH^+} \cdot D_{Cl^-} (z_+ - z_-)}{(z_+ \cdot D_{LidoH^+} - z_- \cdot D_{Cl^-})} \quad (3.25)$$

$D_{LidoH^+}$  for this calculation is assumed essentially equal to  $4.91 \times 10^{-6} \text{ cm}^2/\text{sec}$  corresponding to the undissociated  $D_{Lido}$ . Here  $z_+=+1$ ,  $z_-=-1$  and  $D_{Cl^-} = 2.03 \times 10^{-5} \text{ cm}^2/\text{sec}$  (Newman, 1973), so that

$$D_{LidoH^+Cl^-} = \frac{4.91 \times 10^{-6} \times 2.03 \times 10^{-5} [1 - (-1)]}{4.91 \times 10^{-6} - (-2.03 \times 10^{-5})} = 7.91 \times 10^{-6} \text{ cm}^2/\text{sec}$$

Therefore, the total flux of lidocaine HCl in both forms from Equation (3.24) is:

$$\begin{aligned} J &= (4.91 \times 10^{-6} \times 26 + 7.91 \times 10^{-6} \times 40194) \times 0.50 \times 3600 \\ &\cong 572.5 \mu\text{g}/\text{cm}^2\text{h} \end{aligned}$$

If dimerization existed and its effect were included in the calculation, the model flux would be lower as shown in the calculation for doxycycline HCl.

The flux results from the experimental data appear to be not far from those calculated from the model equations especially for caffeine and lidocaine HCl. If existence of dimerization of lidocaine HCl were considered, the model predictions would probably have been closer to the experimental ones. The deviations are likely to be due to the variations from film to film cut from different parts of a larger piece of film. From these results, it is clear that such a slightly porous polymeric conducting membrane is unlikely to be a major obstacle for these agents to pass through. Therefore, a mouse skin was used next for tests with a PANi membrane on top of it.

### 3.3.2.2 Release Profiles from a Composite of PANi and Mouse Skin Membranes.

The results of the release of three agents through a composite consisting of a PANi membrane with a mouse skin next to it are presented in Figure 3.10. Table 3.10 illustrates the permeation data for each of the three agents. It appears that doxycycline HCl, the

largest molecule, had apparently no release at all. Compared with the data of earlier experiments in 3.2, it is not surprising; without an appropriate enhancer in the donor solution, it is very difficult for doxycycline HCl to go through the mouse skin. For caffeine and lidocaine HCl, the magnitude of the lidocaine HCl concentration (40 mg/ml, higher than that of caffeine, 20mg/ml) is believed to have played a greater role here. Iontophoresis was therefore employed next as an enhancement.

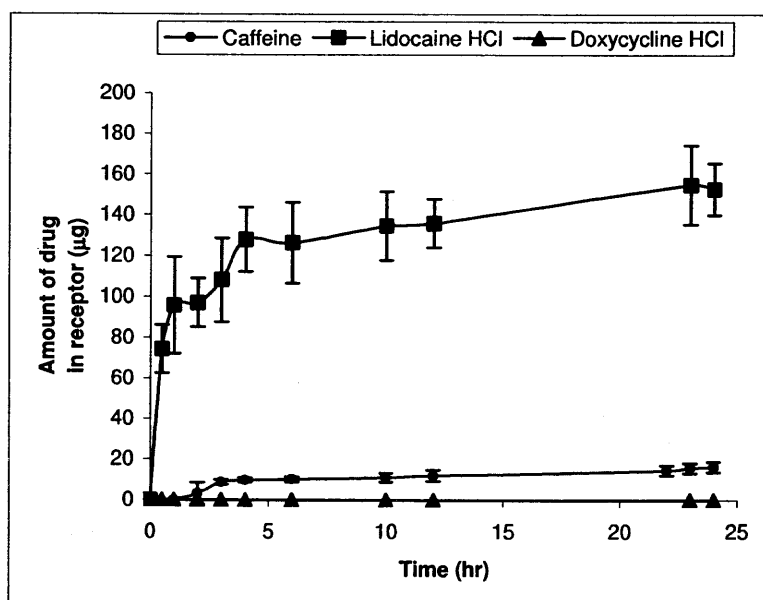


**Figure 3.10** Release profiles of three agents through a composite of PANi and mouse skin membranes.

**Table 3.10** Permeation Data of Three Agents Released through a Composite of PANi and Mouse Skin Membranes

Agent	Permeability (cm/hr)	Flux ( $\mu\text{g}/\text{cm}^2 \text{ hr}$ )	$Q_{24}$ ( $\mu\text{g}/\text{cm}^2$ )
Caffeine	$2.9\text{E-}4 \pm 2.4\text{E-}5$	$7.6 \pm 0.6$	$26 \pm 4$
Lidocaine HCl	$5.0\text{E-}4 \pm 2.5\text{E-}5$	$20.4 \pm 1.0$	$240 \pm 20$
Doxycycline HCl	0	0	0

**3.3.2.3 Iontophoretic Release Profiles from PANi Membranes.** For caffeine and lidocaine HCl, the current density used was  $0.2 \text{ mA/cm}^2$  because of their relatively low MWs; for doxycycline HCl,  $0.3 \text{ mA/cm}^2$  was chosen because its MW is 480.1. To study the iontophoretic property of the PANi membranes, standard Ag|AgCl electrode was used. The results of the release of the three agents are presented in Table 3.11, which illustrates the corresponding permeation data. As for caffeine, a neutral molecule, there was an increase of about 30% in its flux (vis-à-vis Table 3.8), which has been mainly brought about by electroosmosis (Pikal, 1992; Singh et al., 1994; Riviere et al., 1997). For doxycycline HCl, there is over ten times increase in the flux (see Table 3.8), which indicated potentially a promising release behavior if applied on top of a mouse skin. For lidocaine HCl, however, there is a small decrease in the flux.

**Table 3.11** Iontophoretic Permeation Data of Three Agents Released through PANi Film

Agent	Permeability (cm/hr)	Flux ( $\mu\text{g/cm}^2 \text{ hr}$ )	$Q_8^*$ ( $\mu\text{g/cm}^2$ )
Caffeine ( $i=0.2\text{mA/cm}^2$ )	$1.3\text{E}-2 \pm 3.4\text{E}-3$	$310 \pm 80$	$3290 \pm 2400$
Lidocaine HCl ( $i=0.2\text{mA/cm}^2$ )	$1.0\text{E}-2 \pm 3.5\text{E}-3$	$410 \pm 140$	$3080 \pm 1350$
Doxycycline HCl ( $i=0.3\text{mA/cm}^2$ )	$4.0\text{E}-2 \pm 5.6\text{E}-3$	$790 \pm 110$	$2760 \pm 4970$

\* 8 hours accumulation in the receptor part.

According to the Faraday's law, the iontophoretic flux of an ion can be expressed as (Phipps et al., 1989; Banga, 1998)

$$J_i = \frac{t_i i}{FZ_i} \quad (3.26)$$

in which,  $i$ ,  $F$ ,  $t_i$ , and  $Z_i$  are, respectively the applied current density, Faraday's constant, the transport number of ionic species  $i$  and the electrochemical valence of the ion  $i$  under

consideration. To simplify the calculation of  $t_i$ , when the donor part contains only the agent solution without any other ion, the major competing ion with the agent ion is  $Cl^-$ , whose  $t_{Cl^-}$  may be assumed to be 0.86 (Marro et al., 2001). The transport number for the agent ion is then most likely to be 0.14. As for lidocaine HCl, similarly, its cation transport number can be tentatively assumed to be 0.19 (Karami et al., 1997). For the values of the current density applied, and the electrochemical valence for the charge ion, the calculated flux results for lidocaine HCl and doxycycline HCl are shown in Table 3.12; they have also been compared with the experimentally observed values.

**Table 3.12** Comparison of Model Predictions and Experimental Iontophoretic Flux Data

Agent ion	Current density (mA/cm <sup>2</sup> )	Valence $Z_i$	Model prediction ( $\mu\text{g}/\text{cm}^2 \text{ hr}$ )	Experimental flux ( $\mu\text{g}/\text{cm}^2 \text{ hr}$ )
Lidocaine H <sup>+</sup> ion	0.2	1	383	410±140
Doxycycline H <sup>+</sup> ion	0.3	1	752	790±110

For both lidocaine HCl and doxycycline HCl, the experimental values are quite close to the calculated values.

#### 3.3.2.4 Iontophoretic Release Profiles from both PANi and Mouse Skin Membranes.

Three sets of iontophoretic experiments were carried out: in the first set, as a control test, traditional Ag|AgCl electrodes were used for the mouse skin only without the PANi membrane. In the other two sets, with the PANi membrane and the mouse skin together, either PANi|AgCl configuration or the Ag|AgCl configuration as electrodes was tested.

### Lidocaine HCl

The results of three sets of experiments are presented in Figure 3.11. Table 3.13 illustrates the permeation data for the different experimental configurations. The results of the two different sets of electrodes were similar, which indicates that the conducting PANi membrane could be a good replacement for the Ag electrode. And if its properties such as porosity is increased (correspondingly tortuosity is likely to be reduced), it is possible to enhance the flux and accumulation of drug release, i.e., another method of control of transdermal drug delivery.

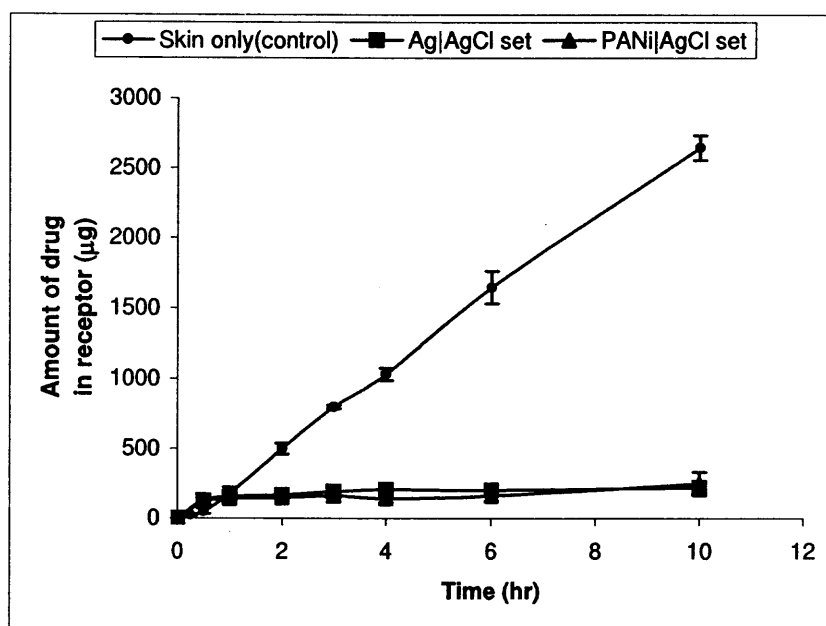


**Figure 3.11** Ionophoretic release profiles of lidocaine HCl through mouse skin with and without a PANi membrane ( $i=0.2 \text{ mA/cm}^2$ ).

**Table 3.13** Iontophoretic Permeation Data of Lidocaine HCl Released through Mouse Skin with and without a PANi Membrane ( $i=0.2 \text{ mA/cm}^2$ )

Set	Permeability (cm/hr)	Flux ( $\mu\text{g/cm}^2 \text{ hr}$ )	$Q_{10}^*$ ( $\mu\text{g/cm}^2$ )
Skin only AglAgCl electrodes	$1.1\text{E-}2 \pm 2.6\text{E-}4$	$430 \pm 10$	$4160 \pm 140$
PANi+skin AglAgCl electrodes	$1.0\text{E-}3 \pm 4.2\text{E-}4$	$48 \pm 20$	$348 \pm 78$
PANi+skin PANiAgCl electrodes	$1.0\text{E-}3 \pm 3.5\text{E-}4$	$43 \pm 15$	$392 \pm 130$

\* 10 hours accumulation in the receptor part.

### Doxycycline HCl

It should be noted that for the sets of PANi membrane and mouse skin together, no release was achieved in the absence of any enhancer added into the donor agent solution. Therefore, instead of using a simple aqueous solution, 5% linoleic acid was added into doxycycline HCl solution made of ethanol and water (EtOH: water=2:1, v/v). The reason for using ethanol was to increase the solubility of linoleic acid into water.

The results of three sets of experiments are presented in Figure 3.12. Table 3.14 illustrates the permeation data for doxycycline HCl under different conditions.

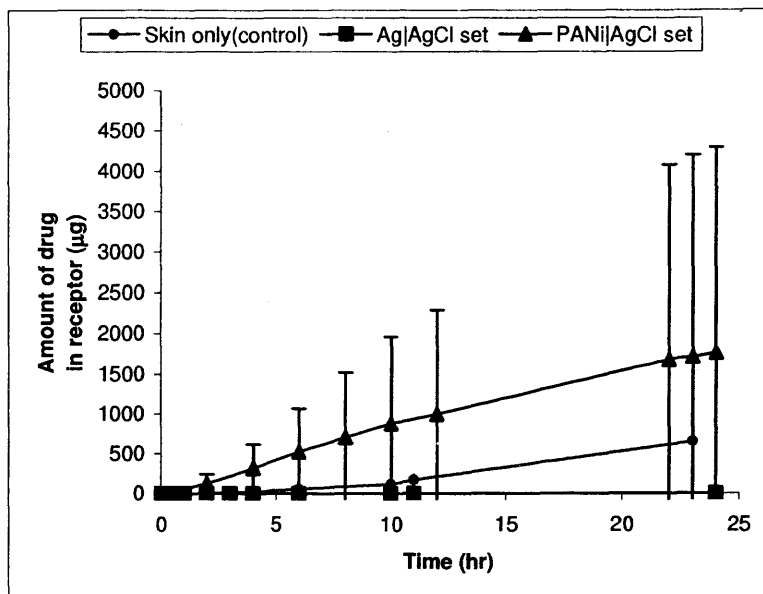


**Figure 3.12** Iontophoretic release profiles of doxycycline HCl through mouse skin with and without a PANi membrane ( $i=0.3 \text{ mA/cm}^2$ ).

**Table 3.14** Iontophoretic Permeation Data of Doxycycline HCl Released through Mouse Skin with and without a PANi Membrane ( $i=0.3 \text{ mA/cm}^2$ )

Set	Permeability (cm/hr)	Flux ( $\mu\text{g/cm}^2 \text{ hr}$ )	$Q_{24}$ ( $\mu\text{g/cm}^2$ )
Skin only Ag AgCl electrodes	$3.8\text{E-}3 \pm 6.7\text{E-}4$	$48.5 \pm 8.5$	$1020 \pm 640$
PANi+skin Ag AgCl electrodes	0	0	0
PANi+skin PANi AgCl electrodes	$5.6\text{E-}3 \pm 4.8\text{E-}3$	$94.4 \pm 81.2$	$2760 \pm 3980$

Unlike the performance of lidocaine HCl, there was no release of doxycycline HCl from the Ag|AgCl electrode set. By the end of the experiment of this set, a white gel-like layer of AgCl was observed on the surface of the PANi film facing the Ag electrode (Figure 3.13). Possibly such deposited matter blocked the pathway for doxycycline HCl to go through the membrane first, and as such nothing came out through the skin. Compared with the lidocaine HCl set, it is believed that with increased ethanol in agent



solution as in the doxycycline HCl solution, increased amount of AgCl was dissolved (Kratohvil et al., 1956; Anderson et al., 1967). However, as shown in the SEM picture of Figure 3.13, such increased solubility of AgCl in the lidocaine case was much smaller in the absence of alcohol; one observes instead individual particles on the PANi film facing the Ag electrode (Figure 3.14). For the PANi/AgCl electrodes set, however, since Ag was not used as electrode, no AgCl blocked the release (Figure 3.15) and the results are even better than those of skin only set due to the enhancements of both iontophoresis and linoleic acid. The high values of deviations could be from the non-homogeneous porous structure of the mounted membranes, which is more important for larger molecules like doxycycline HCl than smaller ones like lidocaine HCl.

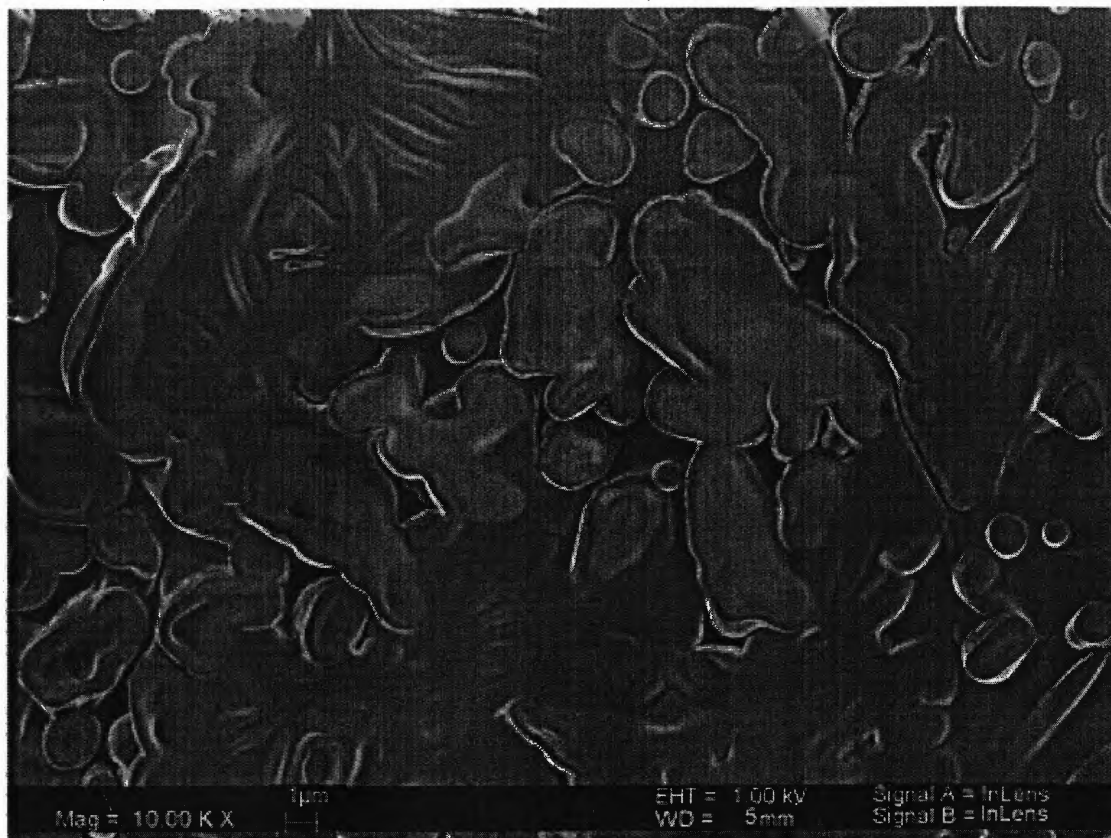


**Figure 3.13** SEM picture of doped PANi film used in the Ag|AgCl set for doxycycline HCl diffusion.

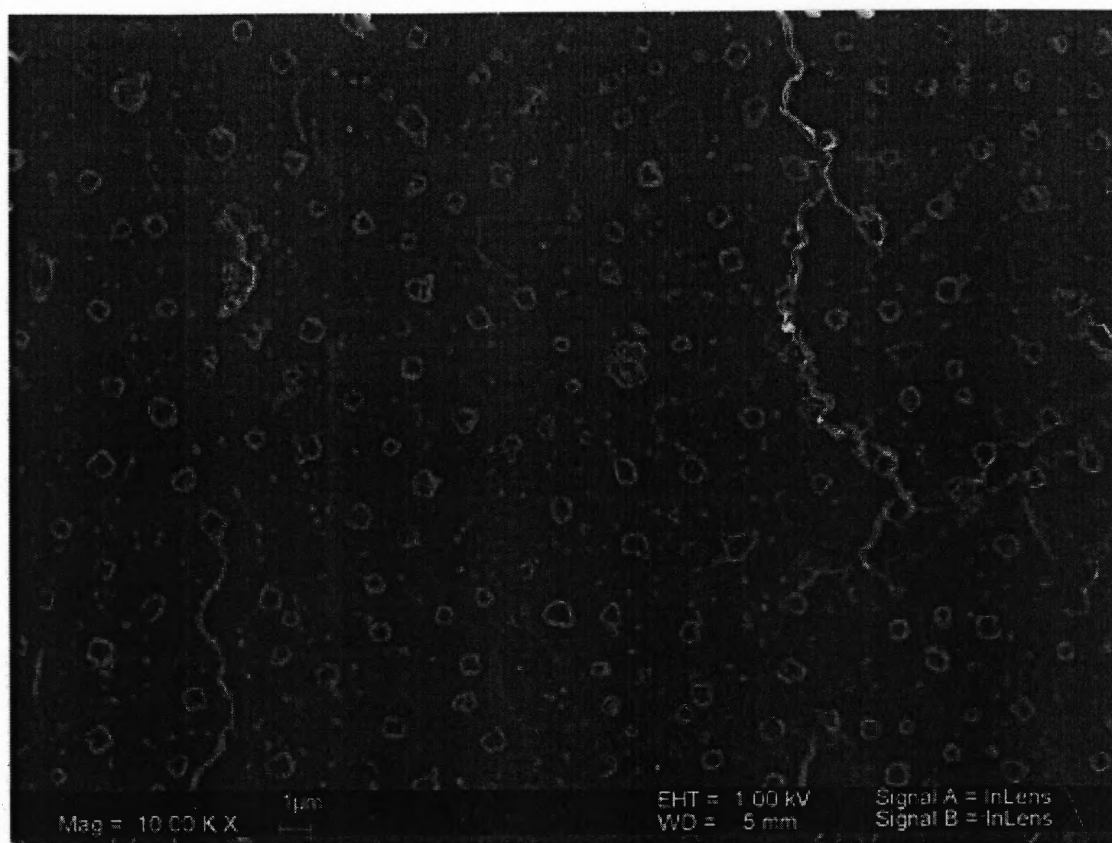


**Figure 3.14** SEM picture of doped PANi film used in the Ag|AgCl set for lidocaine HCl diffusion.

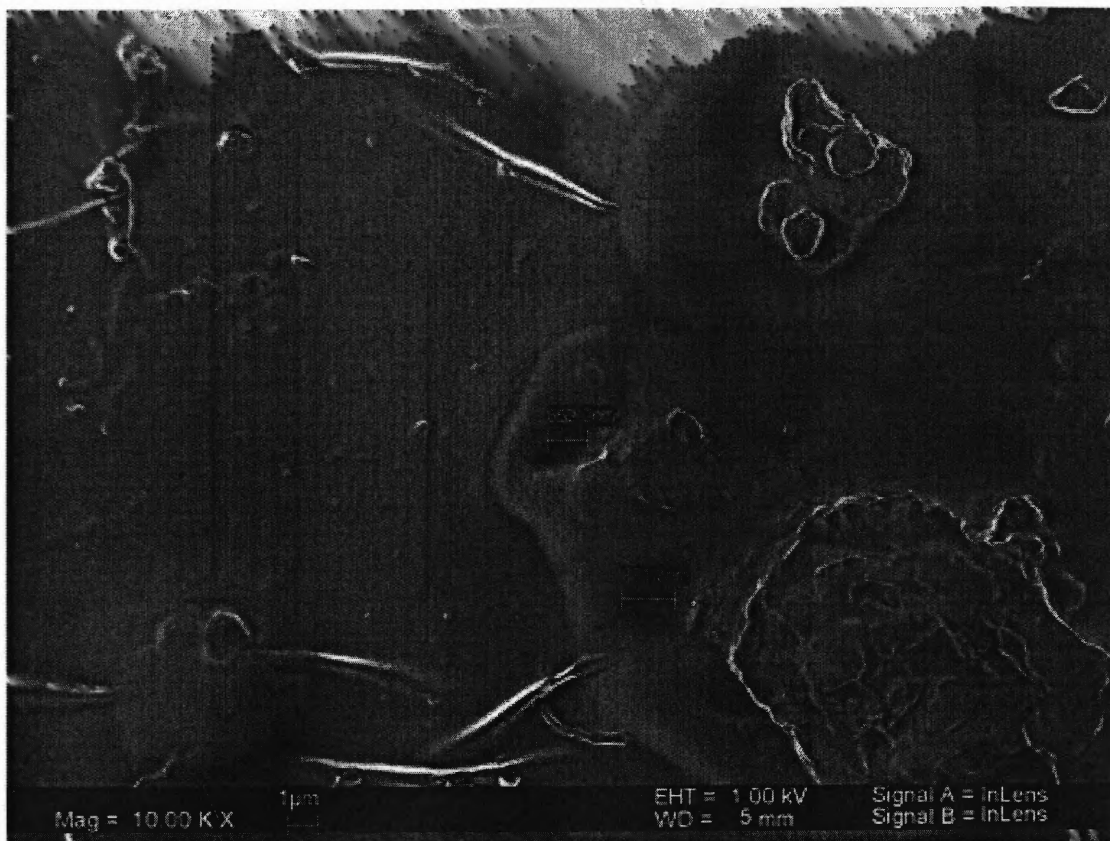


**Figure 3.15** SEM picture of doped PANi film used in the PANi/AgCl set for doxycycline HCl diffusion.

### 3.3.3 Aqueous-Organic Partitioning System

For the permeation study of PANi membrane based on aqueous-organic partitioning system, doxycycline HCl suspension in light mineral oil was used as the donor solution so that its permeation results would be compared with those of PVDF membrane in a general way. Figure 3.16 illustrates the release profile of doxycycline HCl through a PANi membrane based on aqueous-organic partitioning system.

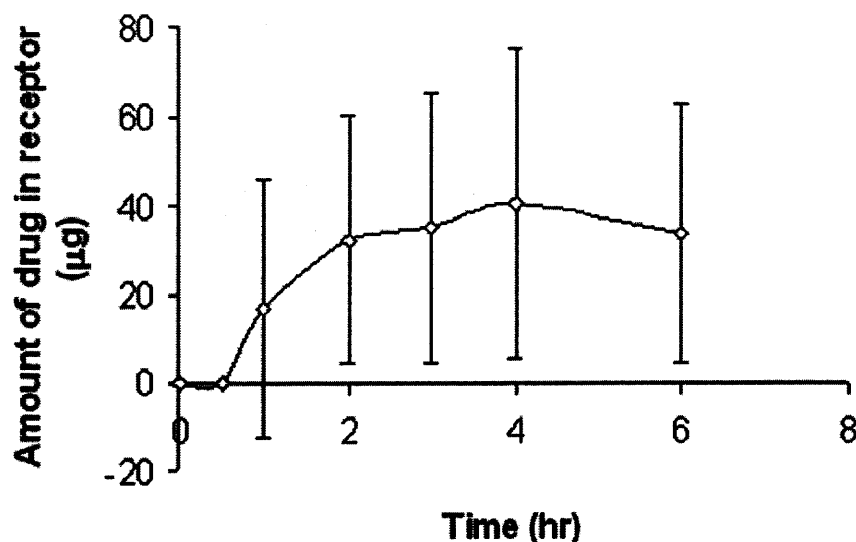


**Figure 3.16** *In vitro* release of doxycycline HCl using light mineral oil as vehicle through PANi membrane over 6 hr.

The permeability, flux and accumulation for six hours of this system were  $0.0031 \pm 0.0018$  cm/hr,  $31 \pm 18$   $\mu\text{g}/\text{cm}^2$  hr and  $80 \pm 46$   $\mu\text{g}/\text{cm}^2$ . Compared to permeation data from aqueous solution in Table 3.8, Section 3.3.2, the permeabilities are close ( $0.0035$  cm/hr from aqueous solution), while the flux ( $72$   $\mu\text{g}/\text{cm}^2$  hr) is more than twice of that from the partitioning system ( $31$   $\mu\text{g}/\text{cm}^2$  hr). Compared to permeation data from PVDF system in Table 3.3, Section 3.1.2, all magnitudes obtained here are much smaller (from PVDF system: P- $0.03$  cm/hr, J- $146$   $\mu\text{g}/\text{cm}^2$  hr). It is believed that the rather small porosity (for PANi, about 1%; for PVDF, 70%) is the primary reason for this low delivery rate. Therefore it would be essential to increase the PANi membrane porosity to further improve delivery from both aqueous solution system and aqueous-organic partitioning system.

### **3.4 Experimental Results of *In Vitro* Delivery of Doxycycline HCl Based on an Aqueous-Organic Partitioning System through a Porous Thermo-Sensitive Membrane and a Mouse Skin**

There were two types of porous thermo-sensitive membranes made: PNIPAAm-immobilized (soaked/coated) thermo-sensitive PVDF membrane (PNIPAAm-PVDF) and PNIPAAm-co-2mol%AA-immobilized (soaked/coated) thermo-sensitive PVDF membrane (2%AA-PVDF). The LCSTs of such thermo-sensitive polymeric gels are presented first. Then doxycycline HCl release profiles from those soaked/coated PVDF membrane alone are illustrated. Permeation through a composite of thermo-sensitive PVDF and mouse skin membranes are presented next. In addition, a relatively small agent, namely, caffeine, was also tested using this thermo-sensitive membrane.

#### **3.4.1 LCSTs of Thermo-Sensitive Polymeric Gels**

The LCSTs of these two gels measured by DSC are about 32.6°C of PNIPAAm (32.6-33.8°C), about 33.0°C of PNIPAAm-co-2%AA (33.0-35.0°C). As described in the introduction, such temperature ranges would match the change of skin temperatures under normal and fever conditions: 32°C as regular one (Bronaugh et al., 1991), and to simplify the different fever temperatures, 33°C is assumed to represent the skin temperature under fever condition.

#### **3.4.2 Release Profiles from Porous Thermo-Sensitive Membrane**

Permeation experiments using doxycycline HCl suspension in light mineral oil as donor solution were carried out at two different temperatures: 32°C mimicing normal skin temperature and 33°C, skin temperature under fever condition.

Figure 3.17 illustrates the polymer synthesis and the final structure. Figures 3.18 and 3.19 show the release profiles from PNIPAAm-PVDF and 2%AA-PVDF at 32°C and 33°C, respectively. Their permeation data are illustrated in Table 3.15.

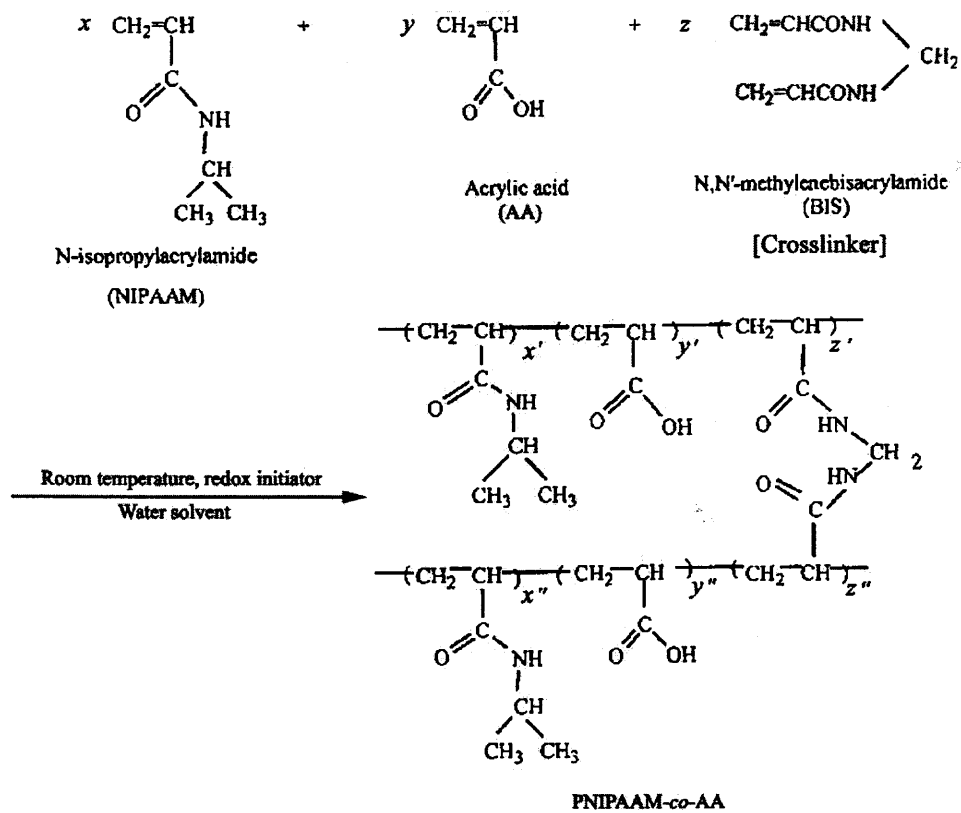
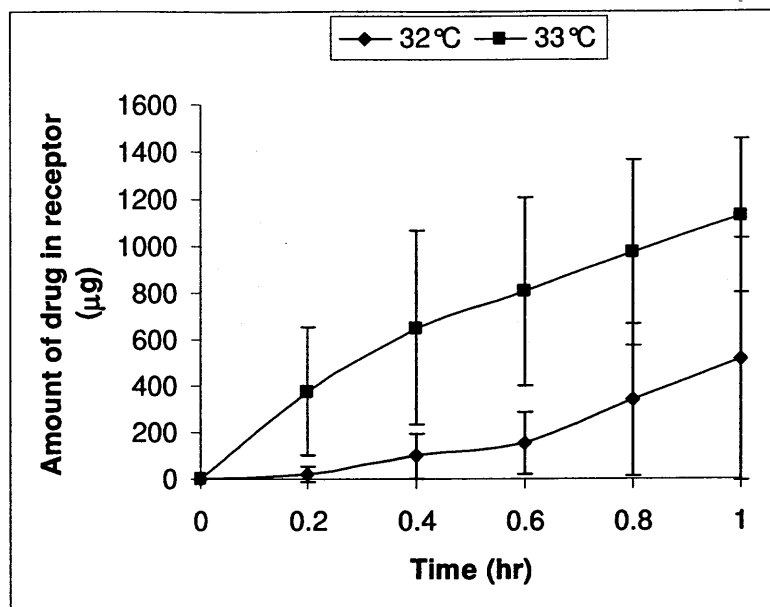
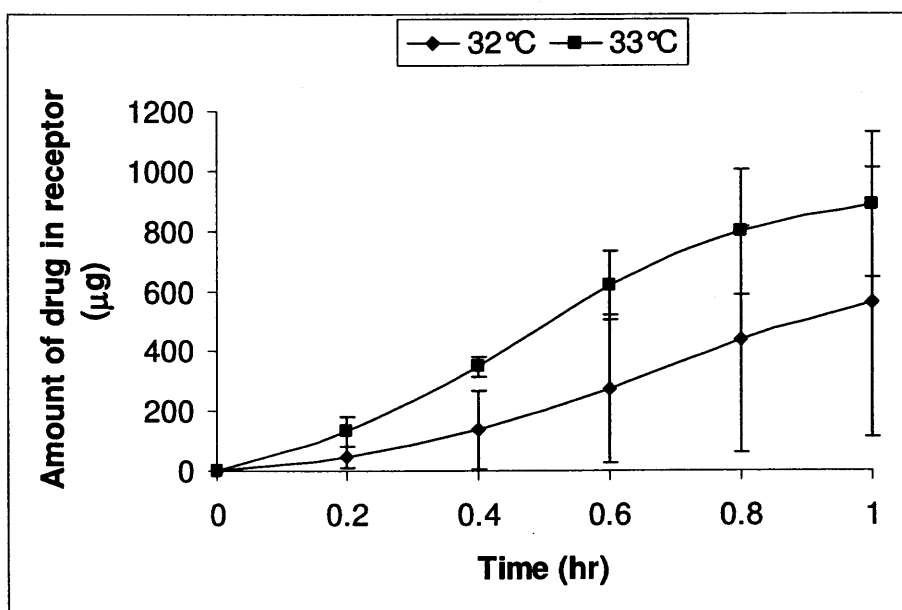


Figure 3.17 Schematic of PNIPAAm-co-AA synthesis.



**Figure 3.18** *In vitro* release of doxycycline HCl using light mineral oil as vehicle through PNIPAAm-PVDF membrane at two temperatures over 1 hr.



**Figure 3.19** *In vitro* release of doxycycline HCl using light mineral oil as vehicle through 2%AA-PVDF membrane at two temperatures over 1 hr.



**Table 3.15** Permeation Data of Doxycycline HCl Released through Different Thermo-Sensitive Membranes at Different Temperatures

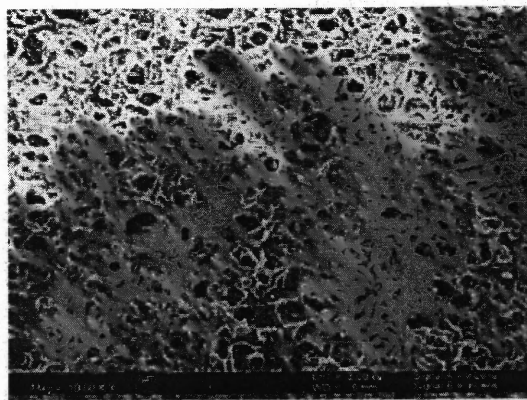
Temp. (°C)	PNIPAAM- PVDF			2%AA -PVDF		
	P (cm/hr)	J ( $\mu\text{g}/\text{cm}^2 \text{ h}$ )	$Q_1^*$ ( $\mu\text{g}/\text{cm}^2$ )	P (cm/hr)	J ( $\mu\text{g}/\text{cm}^2 \text{ h}$ )	$Q_1^*$ ( $\mu\text{g}/\text{cm}^2$ )
32	0.14±0.06	1440±630	1210±590	0.11±0.09	1050±840	880±700
33	0.16±0.03	1560±280	1770±510	0.19±0.06	1900±570	1390±380

\*  $Q_1$ : receptor concentration after 1 hr.

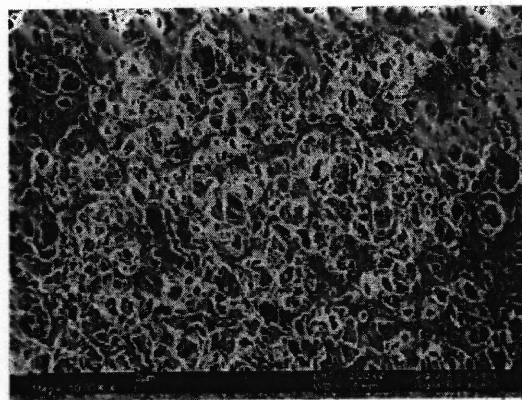
It is obvious that at a higher temperature of 33°C, which is in the range of their phase changing temperatures (LCSTs), both thermo-sensitive PVDF membranes yielded higher permeability, flux and accumulation than those from 32°C, which is below their LCSTs. Figures 3.19 and 3.20 clearly show that the thermo-sensitive gel, either PNIPAAM or PNIPAAM-co-2mol%AA, was both partially coated on the surface of PVDF membrane and penetrated into PVDF membrane pores during synthesis. As described in Chapter 1, it is believed that at a temperature lower than the LCST, e.g., 32°C, the polymer chains are expanded and occupy membrane pores, which partially block the transportation path of doxycycline HCl; when, however, the temperature is raised to 33°C, the polymer underwent a phase change; the chains shrank and condensed to a certain degree (Figure 3.21) (Park et al., 1998), which partially opened the membrane pores so that the system could have an increased permeability, flux and accumulation.



a. Surface image of PVDF membrane without modification

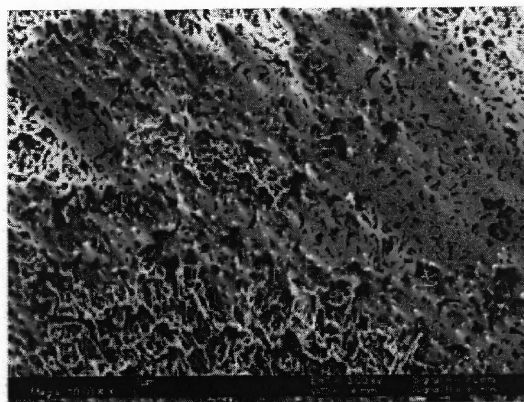


b. Surface image of PNIPAAm-PVDF membrane

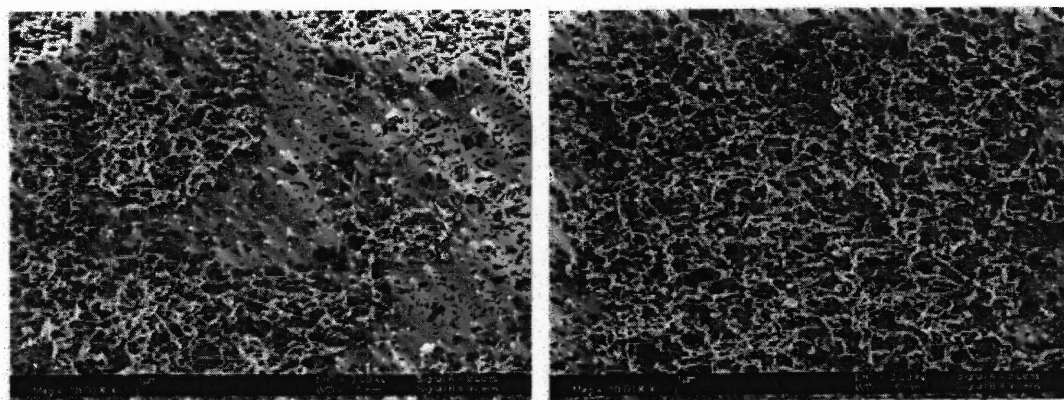


c. Surface image of 2%AA-PVDF membrane

**Figure 3.20** SEM images of PVDF membrane surfaces with and without modification by thermo-sensitive gels.



a. Cross section image of PVDF membrane without modification



b. Cross section image of PNIPAAm-PVDF membrane    c. Cross section image of 2%AA-PVDF membrane

**Figure 3.21** SEM images of PVDF membrane cross section with and without modification by thermo-sensitive gels.

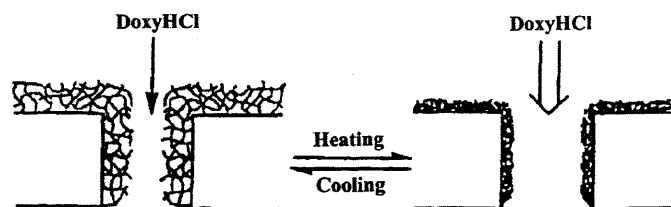


**Figure 3.22** Thermo-sensitive permeation of doxycycline HCl through polymeric gel-immobilized PVDF membrane (Adapted from Park et al., 1998).

From Table 3.15, permeation results from 2%AA-PVDF membrane indicated a much stronger effect of temperature than those from PNIPAAM-PVDF. Therefore, 2%AA-PVDF membrane was selected for study on top of a mouse skin for *in vitro* delivery of doxycycline HCl through a composite of the two membranes.

### 3.4.3 Release Profiles from a Composite of Porous Thermo-Sensitive PVDF and Mouse Skin Membranes

Table 3.16 shows the permeation data of doxycycline HCl release through a composite of 2%AA-PVDF and mouse skin membranes as well as the data from a simple aqueous-organic partitioning system using the same donor solution, enhancer (linoleic acid), PVDF and skin membranes for comparison (Table 3.5, Section 3.2.1).

**Table 3.16** Permeation Data of DoxyHCl through 2%AA-PVDF and Mouse Skin Membranes\*

Configuration	Temperature (°C)	P (cm/hr)	J ( $\mu\text{g}/\text{cm}^2 \text{ h}$ )	$Q_{24}$ ( $\mu\text{g}/\text{cm}^2$ )
2%AA-PVDF + mouse skin	32	0	0	0
	33	$2.6\text{E-}4 \pm 3\text{E-}5$	$2.6 \pm 0.3$	$30 \pm 6$
Regular PVDF + mouse skin	25 (room temp.)	$2.7\text{E-}4 \pm 5\text{E-}5$	$2.7 \pm 0.5$	$63 \pm 9$

\* At the 47<sup>th</sup> hr, DoxyHCl release was detected in the receptor for the 32°C system.

As shown in the Table 3.16, at normal skin temperature, 32°C, there is no release of doxycycline HCl from this system for the first 24 hr; while at 33°C, which represents fever condition, the release data were very close to those from regular PVDF system except the 24 hr accumulation; the deviation in the latter is believed to be due to the following reason: the immobilized thermo-sensitive gel on/into the PVDF membrane increased the lag time of the agent penetration so that it had less time for more agent to go through. However, it did achieve the so called "on-off" switch function as an intelligent polymeric TDD system. It is to be noted that for the release case at 32°C, starting at the 47<sup>th</sup> hr, a small amount of DoxyHCl was also detected from the receptor.

In addition to the permeation of the relatively large molecular weight agent, such as, doxycycline HCl, a smaller agent, namely, caffeine was also studied using such a thermo-sensitive system at two different temperatures. From Figure 3.22, one observes relatively little difference between the two temperatures. Because of the relatively small size of caffeine molecules, one should not expect much difference in the permeation results from two temperatures, i.e., although the membrane pores are partially blocked, it did not impose much resistance to the small molecules (unlike that in the case of 32°C for doxycycline HCl) and only resulted in a smaller porosity. It is possible that with more time, one could achieve the same level of 24-hour accumulation achieved through a regular PVDF membrane and mouse skin.

Figure 3.23 shows the release profiles of caffeine at two different temperatures, and Table 3.17 illustrated their permeation data as well as the data of release through a regular PVDF membrane and mouse skin for comparison.

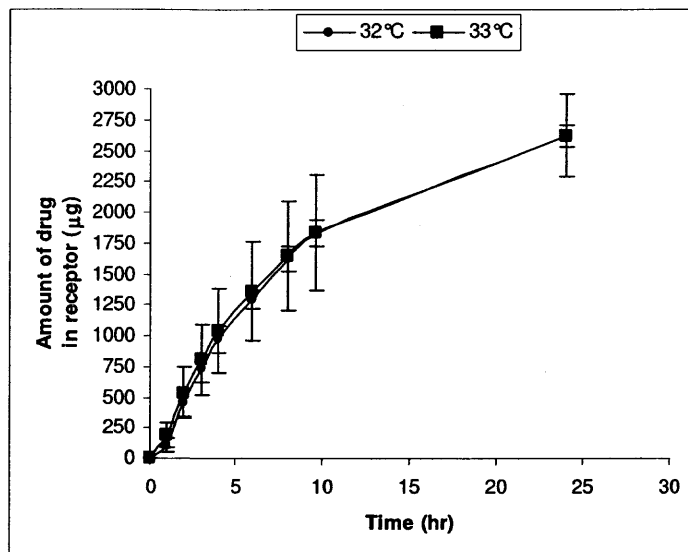


**Figure 3.23** *In vitro* release of caffeine using 1-octanol as vehicle through 2%AA-PVDF membrane at two temperatures over 24 hr.

**Table 3.17** Permeation Data of Caffeine through 2%AA-PVDF and Mouse Skin Membranes

Configuration	Temperature (°C)	P (cm/hr)	J ( $\mu\text{g}/\text{cm}^2 \text{ h}$ )	$Q_{24}$ ( $\mu\text{g}/\text{cm}^2$ )
2%AA-PVDF + mouse skin	32	$0.03 \pm 0.001$	$303 \pm 12$	$4120 \pm 120$
	33	$0.03 \pm 0.002$	$315 \pm 19$	$4120 \pm 530$
Regular PVDF + mouse skin	25 (room temp.)	$0.09 \pm 0.006$	$892 \pm 62$	$4820 \pm 50$

The release profiles and permeation data matched the expectation: at 24<sup>th</sup> hr the thermo-sensitive system did not stop release as the straight line still extended while as Figure 3.8 showed the regular PVDF membrane system almost reached the “plateau” period. There is not much difference in release profiles between 32°C and 33°C: the release lines almost overlapped with each other, and the permeation results of 33°C were just slightly higher than those of 32°C.

Based on the results of two agents: doxycycline HCl (MW: 480) and caffeine (MW: 194), it is clearly indicated that PNIPAAm- and PNIPAAm-co-2mol%AA gel based thermo-sensitive PVDF membrane would function well for relatively large size of agent molecules such as doxycycline HCl; while for small size of agent molecules such as caffeine, other thermo-sensitive polymeric gels might be needed to make PVDF membrane more "dense" at 32°C to minimize the release, or employ certain membranes of small porosity immobilized by PNIPAAm gel to achieve the same goal.

## CHAPTER 4

### CONCLUSIONS AND RECOMMENDATIONS FOR FUTURE STUDIES

#### 4.1 *In Vitro* Drug Delivery Based on an Aqueous-Organic Partitioning System through a Composite of Porous Polymeric and Skin Membranes

The controlled release of a polar antibiotic drug of larger molecular weight i.e., doxycycline HCl using aqueous-organic solute partitioning and microporous polymeric/mouse skin membranes has been studied. The reservoir had either the agent solution in 1-octanol or a dispersion/solution of the agent in light mineral oil. Hydrophobic porous PP Celgard<sup>®</sup> membrane and hydrophilized porous PVDF membranes containing water in the pores were investigated. The transport rates of the agent through such membranes in aqueous-organic partition systems were accurately predicted using appropriate organic-aqueous partition coefficients. After a variety of tests, the porous PVDF membrane and light mineral oil were selected for *in vitro* test. Satisfactory release profiles were achieved not only from the *in vitro* membrane test but also from *in vitro* patch test after its optimization. These demonstrate the practical potential of aqueous-organic partitioning systems and porous membranes to achieve useful controlled release rates. Long term release experiments spanning 120 hours were also carried out and the results were satisfactory. The enhancer linoleic acid was essential to successful release in experiments using the mouse skin.

Agents of smaller molecular weights such as nicotine and caffeine were investigated employing aqueous-organic partitioning and microporous polymeric and mouse skin membranes as well. Without applying any enhancer such as ethanol or linoleic acid needed for the delivery of doxycycline HCl, the transport rates of these



smaller molecules through a mouse skin were quite high: for nicotine (MW: 162), the permeability, flux and 24 hr accumulation were  $0.12 \pm 0.02$  cm/hr,  $1180 \pm 189$   $\mu\text{g}/\text{cm}^2\text{-hr}$  and  $17100 \pm 1520$   $\mu\text{g}/\text{cm}^2$ , respectively; for caffeine (MW: 194):  $0.09 \pm 0.01$  cm/hr,  $892 \pm 62$   $\mu\text{g}/\text{cm}^2\text{-hr}$  and  $4820 \pm 48$   $\mu\text{g}/\text{cm}^2$ , respectively.

Based on the release profiles obtained for these three agents of different molecular weights employing aqueous-organic partitioning and microporous polymeric membrane, satisfactory transdermal drug delivery results were achieved.

#### **4.2 *In Vitro* Iontophoretic Drug Delivery through a Conductive Membrane as an Electrode Placed on a Mouse Skin**

Iontophoretic TDD has been studied using porous membranes of polyaniline, a conducting polymer. Three agents of different molecular weights, caffeine (MW: 194), lidocaine HCl (MW: 271) and doxycycline HCl (MW: 480), were model agents for the tests. Because it is a novel application of PANi membrane in iontophoretic TDD field, the permeation investigation focused first on agents in their aqueous solution. The transport rate of each agent through such a conducting membrane was accurately predicted using simplified mass transport models. Satisfactory release profiles were achieved not only from the *in vitro* membrane test but also from *in vitro* iontophoretic TDD system with a mouse skin. Iontophoresis using PANi|AgCl electrodes presented satisfactory release results. In addition, iontophoretic TDD experiments were performed using both Ag|AgCl electrodes and PANi|AgCl electrodes for comparison. For doxycycline HCl, the flux and 24-hour accumulation from the PANi|AgCl set were  $94.4 \pm 81.2$   $\mu\text{g}/\text{cm}^2\text{-hr}$  and  $2760 \pm 3980$   $\mu\text{g}/\text{cm}^2$ , respectively; those from the Ag|AgCl set were zero. For lidocaine HCl, the flux and 10-hour accumulation from the PANi|AgCl set were, respectively

$43 \pm 15 \mu\text{g}/\text{cm}^2\text{-hr}$  and  $392 \pm 130 \mu\text{g}/\text{cm}^2$ ; the corresponding values from the Ag|AgCl set were  $48 \pm 20 \mu\text{g}/\text{cm}^2\text{-hr}$  and  $348 \pm 78 \mu\text{g}/\text{cm}^2$ . Porous polyaniline membrane appears capable of replacing the Ag part of Ag|AgCl electrode systems; further it can exercise additional control over agent transport rate. As a new material for iontophoretic TDD system, there are many other aspects worthy of additional investigations.

Aqueous-organic partitioning system using the PANi membrane was also studied. However due to the rather low porosity of PANi membrane, the permeation rates were much lower than those from its aqueous solution counterpart; this suggested that future work should focus on making more porous PANi membranes.

#### **4.3 *In Vitro* Drug Delivery through a Porous Thermo-Sensitive Membrane Placed on a Mouse Skin**

The thermo-sensitive membrane, a type of intelligent biomaterial, was synthesized by immobilizing the thermo-sensitive polymeric gel, PNIPAAm or PNIPAAm-co-2mol%AA both on the surface and inside the pores of PVDF membrane. Such a modified membrane has different permeation properties at different temperatures based on the phase changes around its LCST. At  $33^\circ\text{C}$ , which simulates the skin temperature under fever condition, the permeability and flux of 2%AA-PVDF coating ( $0.19 \pm 0.06 \text{ cm/hr}$  and  $1900 \pm 570 \mu\text{g}/\text{cm}^2\text{-hr}$ , respectively) were almost double of those at  $32^\circ\text{C}$  ( $0.11 \pm 0.09 \text{ cm/hr}$  and  $1050 \pm 836 \mu\text{g}/\text{cm}^2\text{-hr}$ , respectively) for the agent doxycycline HCl. Both SEM surface and cross section images of modified PVDF membrane clearly illustrated that there was a thin layer of thermo-sensitive gel coated on the surface, and membrane pores were partially filled with the gel as well, which explains the different permeation rates at different temperatures. Further *in vitro* study with a mouse skin mounted beneath the

thermo-sensitive PVDF membrane demonstrated its release-“on/off” switch function: at 32°C representing normal skin temperature, there was no doxycycline HCl release through skin, while at 33°C, the ailing condition, 30  $\mu\text{g}/\text{cm}^2$  of doxycycline HCl was accumulated in the receptor through the skin after 24 hours with the permeability and flux data being very close to those from the composite of regular PVDF and skin membranes. However, for smaller molecules such as caffeine, different temperatures indicated almost the same permeation profiles.

This part of research simplified and assumed that the normal skin temperature is 32°C, and that under fever conditions is 33°C. In fact, variations of both body and skin temperatures are more complicated. Skin temperatures of different body parts, adults and children vary (Masters, 1980; Suleman et al., 2002). When fever occurs, with less circulation in the capillaries of skin tissue, the skin temperature could even go lower than normal (Silberstein, 1997). Therefore, many other aspects have to be considered in future to make such a thermo-sensitive TDD system more pragmatic and feasible.

#### **4.4 Recommendations for Future Studies**

Successful prediction of the flux values of membrane alone permeation experiments for aqueous-organic partitioning TDD system, and agents in their aqueous solution for iontophoretic TDD system has been achieved based on ion transport, Fick's First Law and the principle of electroneutrality. It would be more meaningful if one can build a mathematical model for the TDD system of a composite of porous polymeric and skin membranes, which would facilitate the selections of both membranes and agents for the optimized formulation and design of transdermal patches.

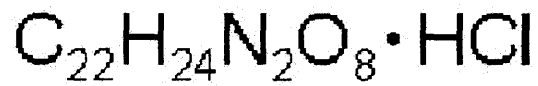
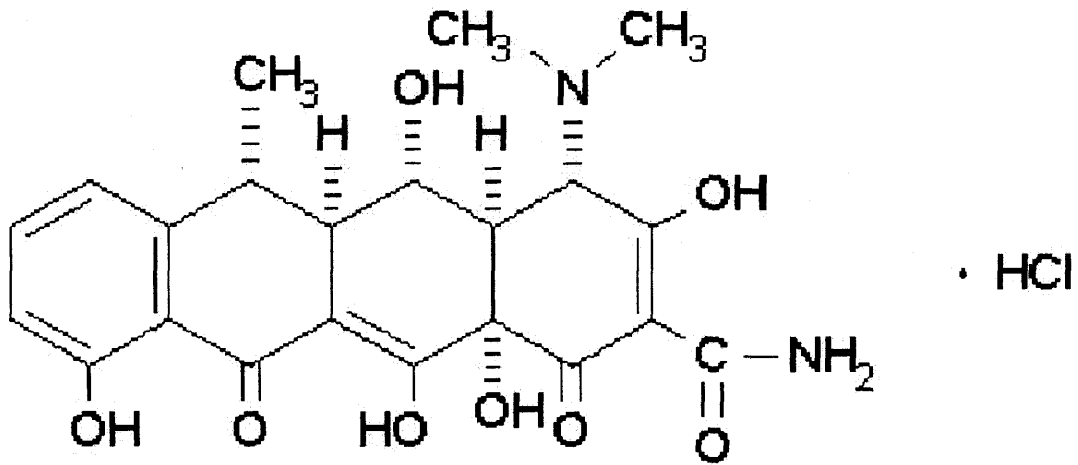
Synthesis of a PANi membrane with a higher porosity would be another challenge. A more porous PANi membrane would yield higher release rate from the aqueous-organic partitioning system. Different porosity would allow this new iontophoretic TDD system control the release rate by both current density and membrane's own property: big dosage of certain drugs could be fulfilled by either higher porosity or higher current density or both and vice versa. In the case of the model prediction (Equation (3.26)), it is clear that properties such as porosity, thickness of membrane used were not involved. It would be another challenge to find out whether those properties would not have an impact on the release profile or were overruled by iontophoresis.

The intelligent TDD system as a thermo-sensitive one reported here is another promising area in the pharmaceutical industry. The PVDF membrane immobilized with the thermo-sensitive PNIPAAm-co-2mol%AA gel worked well for the delivery of doxycycline HCl, a relatively large molecular weight agent; however, for a smaller agent, one still needs to find either another membrane with either smaller pore size or porosity or another thermo-sensitive material to modify it. Therefore, selections of membrane and thermo-sensitive polymers play a great role in successfully delivering different agents. As mentioned above, temperature control is another bigger challenge for this system. Is it possible to customize such a thermo-sensitive transdermal patch based on different sexes, ages, races and different targeting time, sites? It would be great interest to further this aspect of the dissertation work in the future.

## APPENDIX

### STRUCTURE OF DOXYCYCLINE HCL

The chemical structure of doxycycline HCl is illustrated below.



## REFERENCES

- Anderson, K. P., Butler, E. A., Anderson, D. R. & Woolley, E. M. (1967). The solubility of silver chloride and the concentration of silver-containing species in ethanol-water mixtures. Journal of Physical Chemistry, 71, 3566-3569.
- Banga, A. K. (1998). Electrically Assisted Transdermal and Topical Drug Delivery: 172. London, UK: Taylor & Francis Ltd.
- Beronius, P., Dr.; Personal Communication. Sept 13, 2004.
- Bogardus, J. B., Blackwood, R. K., Jr. (1979). Solubility of doxycycline in aqueous solution. Journal of Pharmaceutical Science, 68, 188-194.
- Borodkin, S., Tucker, F. E. (1975). Linear drug release from laminated hydroxypropyl cellulose-polyvinyl acetate films. Journal of Pharmaceutical Science, 64, 1289-1294.
- Bos, J. D., Meinardi, M. (2000). The 500 Dalton rule for the skin penetration of chemical compounds and drugs. Experimental Dermatology, 9, 165-169.
- Bronaugh, R. L., Collier, S. W. (1991). Chapter 19: Protocol for *In Vitro* Percutaneous Absorption Studies. Bronaugh, R. L., Maibach, H., Ed. *In Vitro* Percutaneous Absorption: Principles, Fundamentals, and Applications: 237-241. Boca Raton: CRC Press, Inc.
- Burnette, R. R. (1989). Iontophoresis. Hadgraft, J., Guy, R. H., Ed. *Transdermal Drug Delivery: Developmental Issues and Research Initiatives*. New York City: Marcel Dekker, Inc.
- Chattaraj, S., Walker, R. (1995). Chapter 1.2. Smith, E. W., Maibach, H. I., Ed. *Percutaneous Penetration Enhancers*: 5-15. Boca Raton, FL: CRC press.
- Chen, H., Kovvali, A. S., Majumdar, S. & Sirkar, K. K. (1999). Selective CO<sub>2</sub> separation from CO<sub>2</sub>-N<sub>2</sub> mixtures by immobilized carbonate-glycerol membranes. Industrial and Engineering Chemistry Research, 38, 3489-3498.
- Chien, Y.W. (1982). Novel Drug Delivery Systems: Fundamentals, Developmental Concepts, and Biomedical Assessments. Chapter 2. New York: Marcel Dekker.
- Chong, S., Fung, H-L. (1989). Transdermal drug delivery systems: pharmacokinetics, clinical efficiency, and tolerance development. Hadgraft, J., Guy, R. H., Ed. *Transdermal Drug Delivery: Developmental Issues and Research Initiatives*: 135. New York City: Marcel Dekker.

- El-Kattan, A. F., Asbill, C. S., Kim, N. & Michniak, B. B. (2001). The effects of terpene enhancers on the percutaneous permeation of drugs with different lipophilicities. International Journal of Pharmaceutics, 215, 229-240.
- El-Kattan, A. F., Asbill, C. S. & Michniak, B. B. (2000). The effect of terpene enhancer lipophilicity on the percutaneous permeation of hydrocortisone formulated in HPMC gel systems. International Journal of Pharmaceutics, 198, 179-189.
- Farrell, S. 1996. A Controlled Release Technique Using Microporous Membranes. Ph.D. Dissertation: 192. New Jersey Institute of Technology. Newark, NJ.
- Farrell, S., Sirkar, K. K. (1997). A reservoir-type controlled release device using aqueous-organic partitioning and a porous membrane. Journal of Membrane Science, 130, 265-274.
- Farrell, S., Sirkar, K. K. (1999). A mathematical model of an aqueous-organic partition-based controlled release system using microporous membranes. Journal of Controlled Release, 61, 345-360.
- Farrell, S., Sirkar, K. K. (2001). Mathematical model of a hybrid dispersed network-membrane-based controlled release system. Journal of Controlled Release, 70, 51-61.
- Fischer, W., Haas, R. & Zimmermann, C. 2004. Transdermal delivery system (TDS) with electrode network. U.S. Patent Application Pub. No.: 2004/0193089 A1
- Flynn, G., Smith, R. (1972). Membrane diffusion III: influence of solvent composition and permeant solubility on membrane transport. Journal of Pharmaceutical Science, 61, 61-66.
- Ghosh, B., Reddy, L. H., Kulkarni, R. V. & Khanam, J. (2000). Comparison of skin permeability of drugs in mice and human cadaver skin. Indian Journal of Experimental Biology, 38, 42-45.
- Godwin, D. A., Michniak, B. (1999). Influence of drug lipophilicity on terpenes as transdermal penetration enhancers. Drug Development and Industrial Pharmacy, 25, 905-915.
- Greene, L., Phan, L.X., Schmitt, E.E. & Mohr, J.M. (1993). Side-chain crystallizable polymers for temperature-activated controlled release. El-Nokaly, M.A., Pratt, D.M. & Charpentier, B.A., Ed. Polymeric Delivery Systems: Properties and Applications. Washington, DC: American Chemical Society.
- Grimnes, S. (1984). Pathways of ionic flow through human skin in vivo. Acta Derm Venereol, 64, 93-98.

- Guy, R., Hadgraft, J. (1989). Chapter 3: Selection of Drug Candidates for Transdermal Drug Delivery. Hadgraft, J., Guy, R. H., Ed. Transdermal Drug Delivery: Developmental Issues and Research Initiatives: 59-82. New York: Marcel Dekker.
- Haak, R. P., Theeuwes, F. & Gyory, J. R. 1990. Electrotransport transdermal system. U.S. Patent: 4,927,408
- Helmstadter, A. (2001). The history of electrically-assisted transdermal drug delivery ("iontophoresis"). Pharmazie, 56, 583-587.
- Huglin, M. B., Liu, Y. & Velada, J. L. (1997). Thermoreversible swelling behaviour of hydrogels based on N-isopropylacrylamide with acidic comonomers. Polymer, 38, 5785-5791.
- Kalia, Y. N., Naik, A., Garrison, J. & Guy, R. H. (2004). Iontophoretic drug delivery. Advanced Drug Delivery Review, 56, 619-658.
- Kanikkannan, N. (2002). Iontophoresis-based transdermal delivery systems. BioDrugs, 16, 339-347.
- Karami, K., Sjöberg, H. & Beronius, P. (1997). Ionization conditions for iontophoretic drug delivery. Electrical conductance and aggregation of lidocaine hydrochloride in 1-octanol at 25°C. International Journal of Pharmaceutics, 154, 79-87.
- Kessler, S. B., Klein, E. (1992, 2001). Part IV. Dialysis Chapter 11: Definitions. Ho, W. S., Sirkar, K. K., Ed. Membrane Handbook. Boston: Kluwer Academic.
- Kratohvil, J., Tezak, B. (1956). The influence of the composition and the properties of the solvent on complex formation between silver and chloride, bromide, iodide, and thiocyanate ions. Recueil des Travaux Chimiques des Pays-Bas et de la Belgique, 75, 774-780.
- Kydonieus, A. F., Ed. (1980). Controlled Release Technologies: Methods, Theory and Applications. Boca Raton: CRC Press.
- Langer, R. (1990). New methods of drug delivery. Science, 249, 1527-1533.
- Libinson, G. S. (1977). Doxycycline. Potentiometric titration. Antibiotiki, 22, 1093-1095.
- Lin, P., Zheng, H., Zhang, C., Yang, H., Li, D. & Xu, J. (2003). Preparation of temperature-sensitive polymer with regulated phase transition temperature and its application in the fluoroimmunoassay. Chinese Journal of Analytical Chemistry, 1, 1-4.



- Luyten, M.C., Ekenstein, G.O.R.A. van & Brinke, G. ten (1999). Crystallization and cocrystallization in supramolecular comb copolymer-like systems: blends of poly(4-vinylpyridine) and pentadecylphenol. Macromolecules, *32*, 4404-4410.
- MacDiarmid, A. G., Scherr, E. & Tang, X. 1996. High molecular weight polyaniline films. U.S. Patent: 5,484,884
- Marro, D., Kalia, Y. N., Delgado-Charro, M. B. & Guy, R. H. (2001). Optimizing iontophoretic drug delivery: identification and distribution of the charge-carrying species. Pharmaceutical Research, *18*, 1709-1713.
- Masters, J. E. (1980). Comparison of axillary, oral, and forehead temperature. Archives of Disease in Childhood, *55*, 896-898.
- MMWR (1990). Recommendations for the prevention of malaria among travelers. MMWR Recomm Rep, *39*, 1-10.
- Mogri, Z., Paul, D. R. (2000). Membrane formation techniques for gas permeation measurements for side-chain crystalline polymers. Journal of Membrane Science, *175*, 253-265.
- Mogri, Z., Paul, D. R. (2001). Gas sorption and transport in poly(alkyl (meth)acrylate)s. I. permeation properties. Polymer, *42*, 7765-7780.
- Newman, J. S. (1973). Electrochemical Systems. Table 75-1: 227. Eaglewood Cliffs, New Jersey: Prentice-Hall.
- Panchagnula, R., Pillai, O., Nair, V. B. & Ramarao, P. (2000). Transdermal iontophoresis revisited. Current Opinions in Chemical Biology, *4*, 468-473.
- Park, Y. S., Ito, Y. & Imanishi, Y. (1998). Permeation control through porous membranes immobilized with thermosensitive polymer. Langmuir, *14*, 910-914.
- Parsi, E. J. 1988. Cell for Electrically controlled transdermal drug delivery. U.S. Patent: 4,731,049
- Perkins, N., Heard, C. (1999). In vitro dermal and transdermal delivery of doxycycline from ethanol/migliol 840 vehicles. International Journal of Pharmaceutics, *190*, 155-164.
- Phipps, J. B. 1991. Iontophoresis electrode. U.S. Patent: 5,057,072
- Phipps, J. B. 1992. Iontophoresis electrode. U.S. Patent: 5,084,008
- Phipps, J. B., Padmanabhan, R. V. & Lattin, G. A. (1989). Iontophoretic delivery of model inorganic and drug ions. Journal of Pharmaceutical Science, *78*, 365-369.

- Pikal, M. J. (1992). The role of electroosmotic flow in transdermal iontophoresis. Advanced Drug Delivery Reviews, 9, 201-237.
- Prasad, R., Sirkar, K. K. (1988). Dispersion-free solvent extraction with microporous hollow-fiber modules. AIChE Journal, 44, 177-188.
- Reynolds, J. R., Ly, H. & Kinlen, J. 2002. Burst electrode. U.S. Patent Application Pub. No.: 2002/0022826 A1
- Rhodes III, W. E. (2002). Iontophoretic drug delivery: new advantages revitalize an established technology. Drug Delivery Technology, 2, 34-37.
- Riviere, J. E., Heit, M. C. (1997). Electrically-assisted transdermal drug delivery. Pharmaceutical Research, 14, 687-697.
- Roy, S. D., Hou, S. Y., Witham, S. L. & Flynn, G. L. (1994). Transdermal delivery of narcotic analgesics: comparative metabolism and permeability of human cadaver skin and hairless mouse skin. Journal of Pharmaceutical Science, 83, 1723-1728.
- Sagar, P., Dodddayya, H. (2001). Comparison studies of skin permeability of verapamil HCl transdermal films across mice and human cadaver skin. Indian Drugs, 38, 649-650.
- Sanderson, J. E., Derial, S. R. 1988. Method and apparatus for Iontophoretic drug delivery. U.S. Patent: 4,722,726
- Scott, E. R. 2001. Electrotransport device electrode assembly having lower initial resistance. U.S. Patent: 6,195,582 B1
- Silberstein, W. P. (1997). Fever. Retrieved April 2, 2004 from the World Wide Web: <http://www.mindspring.com/~drwarren/fever.htm>.
- Siman, J., Dove, J. 2001. Medical devices having improved antimicrobial/antithrombogenic properties. U.S. Patent: 6,273,875 B1
- Singh, P., Maibach, H. I. (1994). Iontophoresis in drug delivery: basic principles and applications. Critical Reviews in Therapeutic Drug Carrier Systems, 11, 161-213.
- Sjöberg, H., Karami, K., Beronius, P. & Sundelöf, L. (1996). Ionization conditions for iontophoretic drug delivery. A revised pKa of lidocaine hydrochloride in aqueous solution at 25°C established by precision conductometry. International Journal of Pharmaceutics, 141, 63-70.
- Sloan, K. B., Beall, H. D., Weimar, W. R. & Villanueva, R. (1991). The effect of receptor phase composition on the permeability of hairless mouse skin in diffusion cell experiments. International Journal of Pharmaceutics, 73, 97-104.

- Smith, E., Maibach, H., Eds. (1995). Percutaneous Penetration Enhancers. Boca Raton: CRC Press.
- Suleman, M. I., Doufas, A. G., Akca, O., Ducharme, M. & Sessler, D. I. (2002). Insufficiency in a new temporal-artery thermometer for adult and pediatric patients. Anesthesia & Analgesia, *95*, 67-71.
- Theeuwes, F., Gale, R. & Baker, R. (1976). Transference: A comprehensive parameter governing permeation of solutes through membranes. Journal of Membrane Science, *1*, 3-16.
- Untereker, D. F., Phipps, J. B. & Lattin, G. A. 1992. Iontophoretic drug delivery. U.S. Patent: 5,135,477
- Urquhart, J. 1977. Bandage for transdermally administering scopolamine to prevent nausea. U.S. Patent: 4,031,894
- Urquhart, J. 1981. Method and therapeutic system for administering scopolamine transdermally. U.S. Patent: 4,262,003
- Vander, A. J., Sherman, J. H. & Luciano, D. S. (1994). 6<sup>th</sup> Ed. Chapter 18. Human Physiology: The Mechanisms of Body Function. New York: McGraw-Hill, Inc.
- Vernon, B., Gutowska, A., Kim, S. W. & Bae, Y. H. (1996). Thermally reversible polymer gels for biohybrid artificial pancreas. Macromolecular Symposia, *109*, 155-167.
- Wang, Y., Fan, Q., Song, Y. & Michniak, B. (2003). Effects of fatty acids and iontophoresis on the delivery of midodrine hydrochloride and the structure of human skin. Pharmaceutical Research, *20*, 1612-1618.
- Welty, J. R., Wicks, C. E. & Wilson, R. E. (1976). 2<sup>nd</sup> Ed. Fundamentals of Momentum, Heat, and Mass Transfer. Chapter 30: 634-649. New York: John Wiley & Sons.
- Wen, L., Kocherginsky, N. M. (1999). Doping-dependent ion selectivity of polyaniline membranes. Synthetic Metals, *106*, 19-27.
- Wilke, C. R., Chang, P. (1955). Correlation of diffusion coefficients in dilute solutions. AIChE Journal, *1*, 264-270.
- Yoshida, R., Sakai, K., Okano, T. & Sakurai, Y. (1993). Pulsatile drug delivery systems using hydrogels. Advanced Drug Delivery Reviews, *11*, 85-108.
- Zaffaroni, A. 1976a. Microporous drug delivery device. U.S. Patent: 3,993,072
- Zaffaroni, A. 1976b. Novel drug delivery device. U.S. Patent: 3,993,073